ORIGINAL ARTICLE

Recent progress in TiO₂-based photocatalysts for hydrogen evolution reaction: A review

Ha Huu Do [a,1], **Dang Le Tri Nguyen** [b,1], **Xuan Cuong Nguyen** [b], **Thu-Ha Le** [c],
Thang Phan Nguyen [d,e], **Quang Thang Trinh** [f], **Sang Hyun Ahn** [a], **Dai-Viet N. Vo** [g,*],
Soo Young Kim [h,*], **Quyet Van Le** [b,*]

[a] *School of Chemical Engineering and Materials Science, Chung-Ang University, 84 Heukseok-ro, Dongjak-gu, Seoul 06974, Republic of Korea*
[b] *Institute of Research and Development, Duy Tan University, Da Nang 550000, Vietnam*
[c] *Faculty of Materials Technology, Ho Chi Minh City University of Technology (HCMUT), Vietnam National University–Ho Chi Minh City (VNU–HCM), 268 Ly Thuong Kiet, District 10, Ho Chi Minh City, Vietnam*
[d] *Laboratory of Advanced Materials Chemistry, Advanced Institute of Materials Science, Ton Duc Thang University, Ho Chi Minh City, Vietnam*
[e] *Faculty of Applied Sciences, Ton Duc Thang University, Ho Chi Minh City, Vietnam*
[f] *Cambridge Centre for Advanced Research and Education in Singapore (CARES), Campus for Research Excellence and Technological Enterprise (CREATE), 1 Create Way, 138602, Singapore*
[g] *Center of Excellence for Green Energy and Environmental Nanomaterials (CE@GrEEN), Nguyen Tat Thanh University, 300A Nguyen Tat Thanh, District 4, Ho Chi Minh City 755414, Vietnam*
[h] *Department of Materials Science and Engineering, Korea University, 145 Anam-ro Seongbuk-gu, Seoul 02841, Republic of Korea*

Abstract TiO₂ has gained tremendous attention as a cutting-edge material for application in photocatalysis. The performance of TiO₂ as a photocatalyst depends on various parameters including morphology, surface area, and crystallinity. Although TiO₂ has shown good catalytic activity in various catalysis systems, the performance of TiO₂ as a photocatalyst is generally limited due to its low conductivity and a wide optical bandgap. Numerous different studies have been devoted to overcome these problems, showing significant improvement in photocatalytic performance. In this study, we summarize the recent progress in the utilization of TiO₂ for the photocatalytic hydrogen evolution reaction (HER). Strategies for modulating the properties toward the high photocat-

* Corresponding authors.
 E-mail addresses: nguyenphanthang@tdtu.edu.vn (T.P. Nguyen), daivietvnn@yahoo.com (D.-V.N. Vo), sooyoungkim@korea.ac.kr (S.Y. Kim), levanquyet@dtu.edu.vn (Q.V. Le).
 [1] Ha Huu Do and Dang Le Tri Nguyen equally contributed to this work.
Peer review under responsibility of King Saud University.

alytic activity of TiO_2 for HER including structural engineering, compositional engineering, and doping are highlighted and discussed. The advantages and limitations of each modification approach are reviewed. Finally, the remaining obstacles and perspective for the development of TiO_2 as photocatalysts toward high efficient HER in the near future are also provided.

1. Introduction

Currently, the world faces unprecedented challenges concerning energy and environmental topics. The use of nonrenewable fossil fuel to meet the daily energy demands has released a huge amount of CO_2 gas compares with renewable energies (Fig. 1), contributing to global warming as well as air pollution (Pao and Tsai, 2010). Hydrogen is considered as an ideal solution to tackle this problem, owing to its sustainable, energy-dense, and eco-friendly properties (Baykara, 2018, Catapan et al., 2018, Im et al., 2009). It is utilized in a wide variety of applications, including petroleum refining, electric production, gas welding, automobile fuel, and rocket fuel for space programs (Staffell et al., 2019; Tusek and Suban, 2000). Several countries such as China, Britain, and the United States have used hydrogen as an alternative fuel for transportation to reduce greenhouse gas emissions in large cities (Zhu et al., 2018). Thus, finding a simple and efficient method to manufacture hydrogen is necessary. Commercial hydrogen can be manufactured using various approaches such as gasification of coal, steam reforming of natural gas, cryogenic distillation process, and water splitting (Haryanto et al., 2005). Among these methods, water splitting has attained economic and environmental efficiency, owing to several reasons. The first two methods can generate a large amount of hydrogen. However, these methods required high energy consumption (temperature > 1000 °C) to conduct reactions, demanding a robust and safe system. The third method is based on the various boiling points of gaseous which require extremely low temperature. Whereas, the separation of water can be implemented at ambient temperature and pressure, thus, lowering the production costs. However, utilizing large amounts of electric energy to produce hydrogen from water leads to the limitation of electrocatalytic water splitting. Therefore, the use of photocatalyst to create hydrogen from water is a reasonable solution to reduce the cost of manufacture in particular utilization, owing to solar energy. Accordingly, numerous studies on potential photocatalysts have focused on the hydrogen evolution reaction (HER), such as metal–organic frameworks (MOFs) (Chen et al., 2017; Silva et al., 2010; He et al., 2013; Jayaramulu et al., 2016, Liu et al., 2017; Santaclara et al., 2017; Wen et al., 2016; Zhang et al., 2015a,b; Zhen et al., 2016), carbon nitrides (Bai et al., 2018; Cao and Yu, 2014; Chen et al., 2018; Dong et al., 2013; Fang et al., 2019; Guo et al., 2018; Hou et al., 2013; Li et al., 2015a,b,c; Wang et al., 2018; Wang et al., 2012), and graphene (Iwase et al., 2011; Min and Lu, 2012; Zhang et al., 2012). Amongst the promising photocatalysts, TiO_2 is considered as a typical material for potential applications in photocatalysis, owing to its high stability, nontoxicity, reasonable cost, and
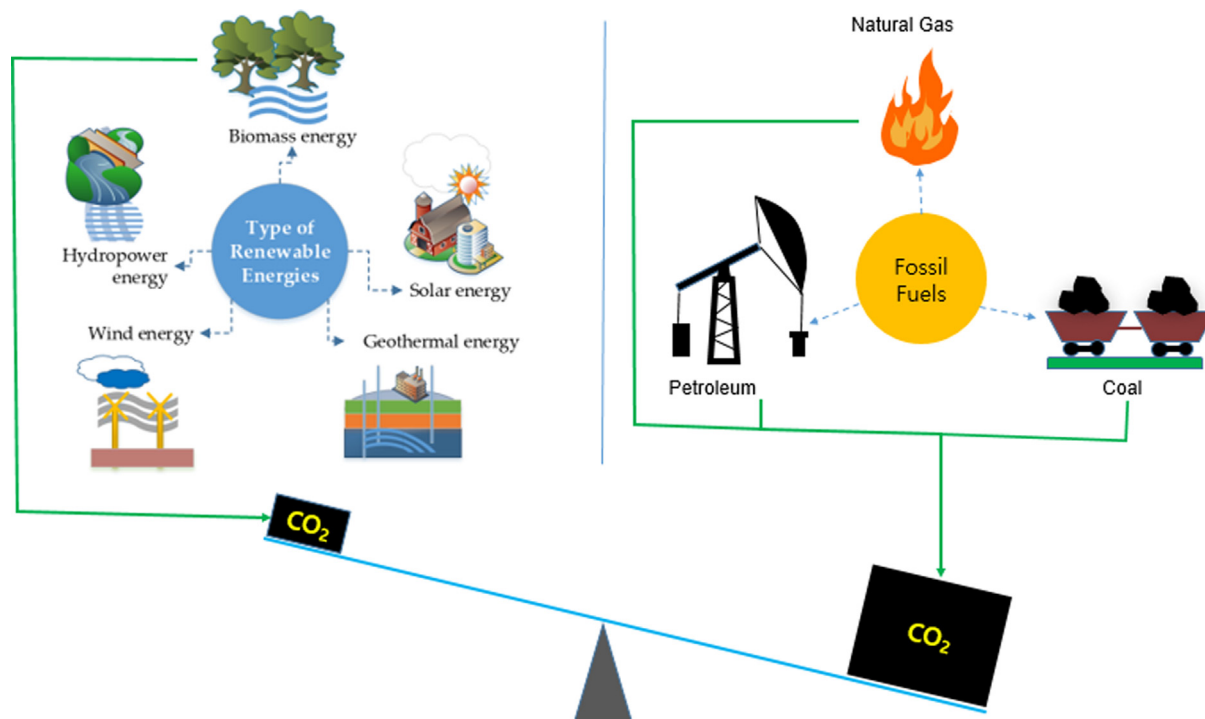
Fig. 1 A represented diagram for generating CO_2 from fossil fuels and renewable energies (Avtar et al., 2019).

eco-friendliness (Chen et al., 2016a, b; Rossetti et al., 2015; Hong et al., 2018). Traditionally, anatase and rutile have gained a great deal of interest in the photocatalytic field. The two phases of TiO$_2$ most commonly used in photocatalysis are anatase and rutile. Because it has good optical absorption capacity and low cost, several studies have indicated that anatase is more efficient than rutile for catalyzing reaction under solar light, although its experimental bandgap (E$_g$ = 3.2 eV) is broader than that of rutile (E$_g$ = 3.0 eV) (Alkaim et al., 2013). The enhanced catalytic activity is accounted for the high-density hydroxyl species on the surface as well as the large surface area. Hydroxyl groups are crucial to prohibit the reconsolidation of electron–hole pairs, and the great specific surface area creates conducive conditions for the absorption of the reactant on the surface of catalyst, playing a pivotal role in photocatalytic reactions (Chen et al., 2015; Pang et al., 2014). Some studies scrutinized the domination of internal factors on the yield of TiO$_2$ in the photocatalytic area (Yamazaki et al., 2018). For instance, Yamazaki et al. investigated the importance of a morphological change of TiO$_2$ from nanorods (NRs) to nanoparticles (NPs) on the photocatalytic performance for the oxygen evolution reaction (Cheng et al., 2014; Liu et al., 2014a,b; Suhaimy et al., 2018; Yamazaki et al., 2018). Cheng's study indicated that the specific surface area of TiO$_2$ is crucial in photocatalytic applications (Cheng et al., 2014). Generally, the catalytic activity of TiO$_2$ is governed by various parameter including the specific surface area, crystallinity, and morphology. However, the large bandgap width and low conductivity cause difficulty in the exciton dissociation and electron transfer, which restricts the potential applications of TiO$_2$. Thus, some strategies were employed to modify TiO$_2$ to reduce its bandgap and increase its conductivity. For example, the bandgap of TiO$_2$ was effectively reduced through replacing titanium or oxygen atoms in TiO$_2$ lattice with metal and nonmetal dopants (Bakar and Ribeiro, 2016; Hou et al., 2014; Koči et al., 2010; McManamon et al., 2015; Sood et al., 2015; Wu et al., 2013). Another method is to modify the surface of TiO$_2$ by an inorganic acid such as H$_2$SO$_4$ to generate hydroxyl groups on the surface of TiO$_2$, vacancies, and intensify the light absorption efficiency (Li et al., 2015a, b,c). Moreover, the combination of TiO$_2$ with advanced materials such as carbon based materials, transitional metal dichalcogenides (TMDs), metal oxides, and metal-organic frameworks (MOFs) were also investigated to promote the photocatalytic activity of TiO$_2$ toward the HER (Majeed et al., 2017; Xiang et al., 2012). For example, graphene has unique electronic and optical properties, with zero bandgap (Kim et al., 2016; Park et al., 2017; Zheng et al., 2018). Therefore, the incorporation of graphene into TiO$_2$ not only increases the electrical conductivity but also reduces titania's bandgap, thus improving the overall performance of the catalysts. Apart from graphene, other 2D materials such as TMDs, and transition metal carbides are also expected to be excellent in combination with TiO$_2$. Moreover, MOFs, which are known as porous crystalline materials with outstanding features including large specific surface area, high thermal stability, adjustable structural components, have also been rationally investigated by means of forming composite catalysts with TiO$_2$ for the HER (Antwi-Baah and Liu, 2018; Farha et al., 2012; Xia et al., 2015).

Herein, we highlight the recent finding in the utilization of TiO$_2$ for solar water splitting. Strategies for modulating the key features toward the high performance of TiO$_2$ for the HER, including structural engineering, compositional engineering, and doping are highlighted and discussed. The advantages and limitations of each modification approach are reviewed. Finally, the existing approaches and possibilities for the improvement of TiO$_2$ as photocatalysts are provided.

2. TiO$_2$-based photocatalysts for HER

2.1. Fundamental of photocatalytic HER

The separation of water takes place under UV, visible, or UV–Vis irradiation, including several principal steps (Fig. 2) (Jafari et al., 2016). First, a photocatalyst absorbs solar energy that is equal to or greater than the bandgap of TiO$_2$ to form excitons. Second, as a result, the electron moves from the valence band (VB) to the conduction band (CB) while the hole remains in the VB. Third, protons that adsorbed on the surface of TiO$_2$ received the new generated electron to produce hydrogen (Eq. (1)) and water is oxidized by the holes to form oxygen (Eq. (2)).

$$2H^+ + 2e^- \rightarrow H_2 \ E^0 = 0.00 \ eV \tag{1}$$

$$H_2O + 2 \ h^+ \rightarrow 2H^+ + 1/2O_2 \ E^0 = 1.23 \ eV \tag{2}$$
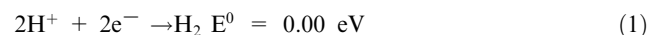
The initial condition for a reaction under the light resource is that the catalyst has a value of CB, which is smaller than the reduction potential of H$^+$/H$_2$ (0 eV) and its VB level larger than the reduction potential of O$_2$/H$_2$O (1.23 eV). Therefore, TiO$_2$ is a promising candidate for a photocatalytic HER with a CB level of −0.3 eV and a VB level of 2.9 eV. TiO$_2$ as a catalyst for solar water splitting was first reported by Fujishima and Honda (Fujishima and Honda, 1972). The photocatalytic experiments were evaluated under UV light in a photoelectrochemical system with TiO$_2$ as an anode and platinum as a cathode. Oxygen was released on the facade of TiO$_2$ and hydrogen was exhausted from the Pt electrode. This result paved the way for the photocatalytic field. However, with a large original bandgap, TiO$_2$ is only photoactive under the UV light, which accounts for 4% of solar energy. Moreover, a subprocess usually appears in the photoreduction reaction, which is a reconsolidation of charge pairs, leading to go down catalytic efficiency. To overcome these challenges, several campaigns have been implemented to promote the photocatalytic activity of TiO$_2$ for the HER.

2.2. TiO$_2$ photocatalyst for HER

2.2.1. Structural engineering
2.2.1.1. TiO$_2$ nanostructure engineering. TiO$_2$ is a well-known n-type inorganic semiconductor. Therefore, it can pair with p-type semiconductor such as p-Si to form a p-n heterojunction structure which expedites the electron moving from p-Si through TiO$_2$ to active sites. For example, Andoshe et al. fabricated TiO$_2$ nanorods on a p-type silicon plate as a cathode material for photocatalytic water splitting (Andoshe et al., 2016). TiO$_2$ NRs/p-Si were created through a hydrothermal process with tetrabutoxytitanium as a precursor. The use of TiO$_2$ substantially increased the optical absorption of p-Si
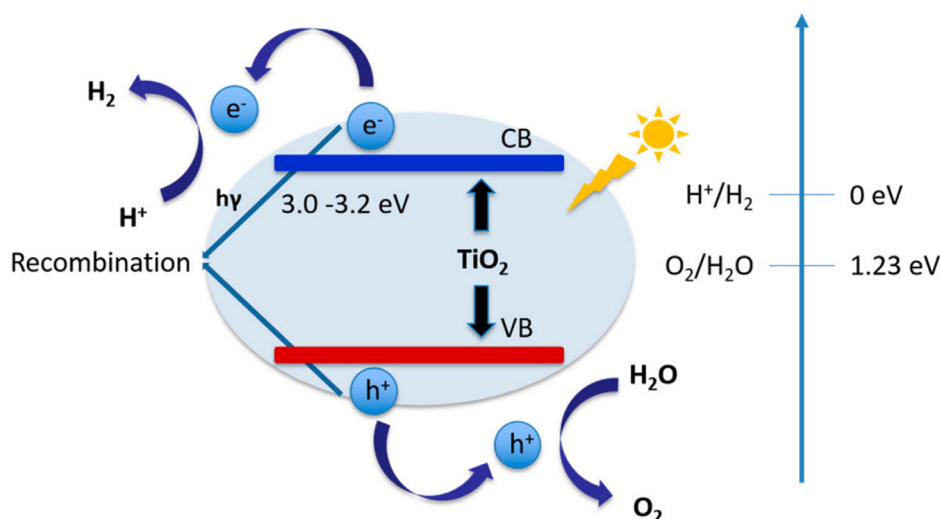
Fig. 2 Schematic illustration of TiO$_2$ for photocatalytic hydrogen evolution reaction (Jafari et al., 2016).

sample. The evidence is that the reflectance values measured at 550 nm are 37.5% and 1.4% for p-Si and TiO$_2$ NRs/p-Si pattern, respectively. Besides, TiO$_2$ NRs/p-Si also has better light absorption than TiO$_2$ seed layer/p-Si. As a result, when Pt nanoparticles were deposited on these samples, the photoelectrochemical (PEC) performance was remarkably enhanced. A saturation current density as high as 40 mA cm^{-2}, an onset potential approximately 440 mV, given by Pt-TiO$_2$ NRs/p-Si sample. Furthermore, heterojunction devices are durable over 52-hours test. Another finding based on TiO$_2$ NRs was reported by Yoon et al. (2019). In short, MIL(125)–NH$_2$ was deposited on the surface of TiO$_2$ NRs, which flourished on FTO/glass pattern. This device operated as an anode for separating of water under solar energy. Catalytic performance was evaluated in alkaline solution (pOH = 0.4) under AM 1.5 G irradiation. The outcome reveals that a photocurrent density of 1.63 mA/cm^2 at 1.23 V vs RHE was observed. This value is about 3-time higher than that of the bare TiO$_2$ NRs. There are some factors contribute for this finding, including large specific surface area and high crystallinity of TiO$_2$ NRs and an appropriate bandgap width of MOF (MIL(125)–NH$_2$). Specially, the combination of MIL(125)–NH$_2$ and TiO$_2$ NRs generated a type (II) heterojunction structure, which facilities the electron transport to the active area for HER.

Besides, mesoporous TiO$_2$ materials have attracted increasing attention in photocatalytic applications owing to their outstanding properties such as low cost, high stability, good electronic structure, and optical features. Many studies have been conducted to enhance the photocatalytic activity of mesoporous TiO$_2$ materials. Two structures, involving rutile mesoporous single-crystal NRs (R-MSC) and anatase mesoporous single crystal nanosheets (A-MSC) were synthesized and investigated for their photocatalytic activity in water splitting (Fig. 3a) (Zheng et al., 2013). The morphology and size of mesoporous TiO$_2$ were mainly affected by three factors, including the seeding concentration, hydrohalic acid condition, and temperature. The study results revealed that rutile mesoporous single-crystal NRs with a seeding concentration of 0.3 mM (R-MSC-0.3) showed the best photocatalytic performance for hydrogen generation from water, which is much higher than of rutile single-crystal (R-SC). The same tendency

occurred for A-MSC-0.3 and A-SC (Fig. 3b). The promoted catalytic activity was attributed to the increased specific surface area and the monocrystalline solid. In addition, the facets of R-MSC are active centers, having an important role in photocatalytic reactions (Fig. 3c). With the tunability of the structure as well as the model, mesoporous TiO$_2$ has many prospective applications in the field of photocatalysis.

2.2.1.2. Black TiO$_2$. Initially, Chen *et al.* synthesized black TiO$_2$ from white TiO$_2$ through a hydrogenation process for hydrogen production (Chen et al., 2011). The result indicated that the optical absorption range of black TiO$_2$ is wider than that of white TiO$_2$. As a result, black TiO$_2$ has a higher photocatalytic yield than that of white TiO$_2$. This is a breakthrough in the use of TiO$_2$ for photocatalytic water splitting. Therefore, many research groups have followed this direction to promote the catalytic activity of TiO$_2$ in potential applications. For example, Wang *et al.* fabricated a core–shell black TiO$_2$ structure by a hydrogen plasma method for catalyzing the HER (Wang et al., 2013). This material showed a hydrogen production rate per mass unit of 10 mmol h^{-1} g^{-1}. This rate is much higher than the value of pristine TiO$_2$. However, the black TiO$_2$ has a low porosity with a surface area of less than 50 m^2 g^{-1}. To tackle this problem, Zhou *et al.* found a new technique to fabricate an ordered mesoporous TiO$_2$ (OMT) with an ethylenediamine encircling step before hydrogenation was performed to achieve an ordered mesoporous black TiO$_2$ (OMBT) (Fig. 4a) (Zhou et al., 2014). The morphology of OMBT can be observed by transmission electron microscopy (TEM) in Fig. 4(b,c). The obtained OMBT exhibited a high specific surface area of 124 m^2 g^{-1}, a high crystallinity, and a wide range of light from the UV–Vis to the infrared region. Besides, the separation and lifetime of photoinduced charges were substantially increased, leading to improved catalytic activity of OMBT structures. As a consequence, OMBT materials showed a hydrogen production rate of 136.2 μmol h^{-1} which is nearly 2-fold higher than that of original OMT (76.6 μmol h^{-1}) under a standard light source (AM 1.5) (see Fig. 4d). In addition, catalytic stability of OMBT was maintained over 30 h test.
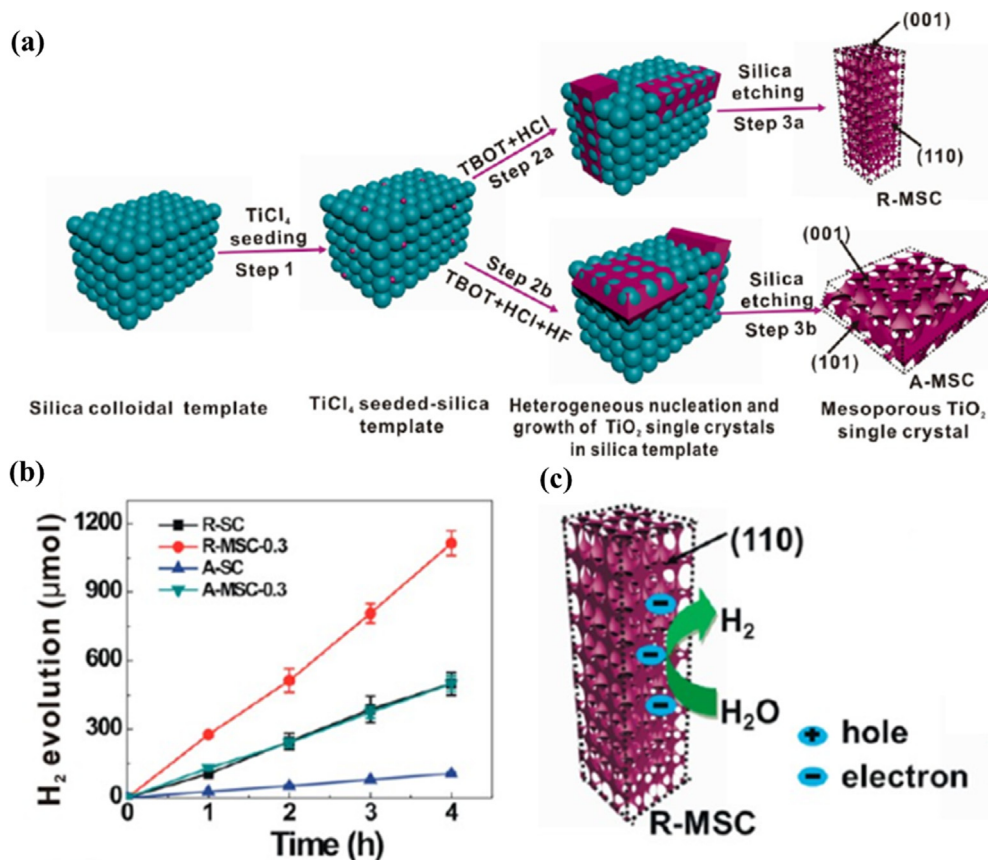
Fig. 3 (a) Schematic diagram of the synthesis of R-MSC and A-MSC in silica template. (b) Comparison of H$_2$ formation rate by different catalysts. (c) The proposed mechanism for photocatalytic hydrogen evolution on R-MSC (Xiaoli Zheng et al., 2013).
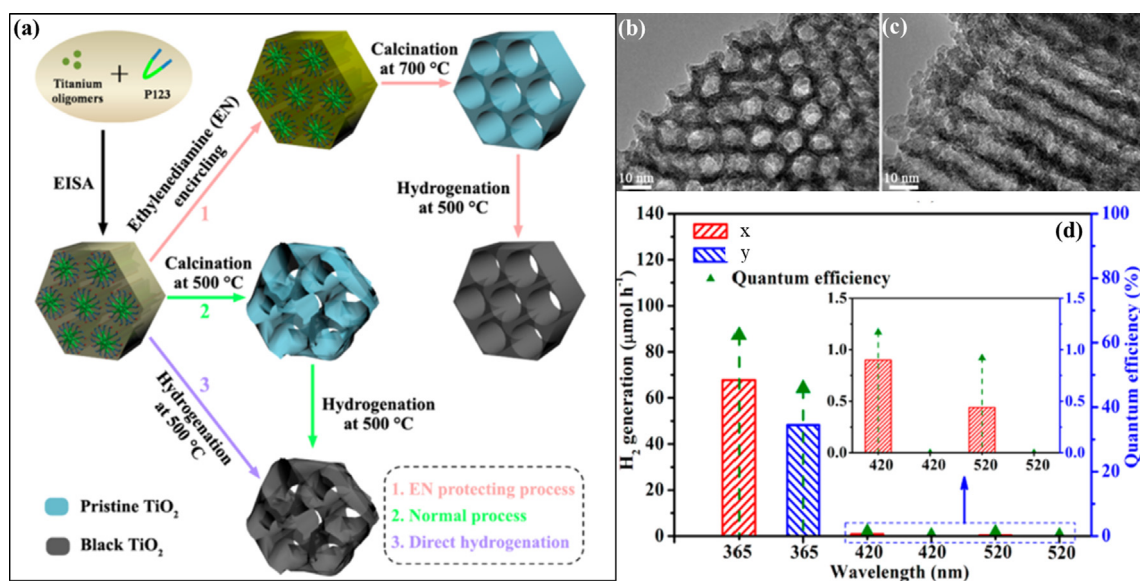
Fig. 4 (a) Representation of the fabrication of ordered mesoporous black TiO$_2$ materials. Illustrative TEM images along (b) [1 0 0] (c) [1 1 0]. (d) The photocatalytic hydrogen production rate of ordered mesoporous black TiO$_2$ (x) and pristine ordered mesoporous TiO$_2$ materials (y) (Zhou et al., 2014).

2.2.2. Compositional engineering

2.2.2.1. Graphene/TiO$_2$ composites.

The invention of graphene opened a new chapter in the scientific field. Graphene is the first two-dimensional material with outstanding characteristics such as high specific surface area and good electron transferability, which minimize the reconsolidation of photogenerated charges to enhance the photocatalytic yield of the material. Graphene does not have any bandgap, whereas the bandgap of TiO$_2$ is large. Therefore, the incorporation of graphene and TiO$_2$ is considered as a perfect couple for photocatalytic applications. This was first reported for photocatalytic hydrogen production by Zhang et al. (2010). Graphene sheets (GSs)/TiO$_2$ composites with the different ratios were created via a simple sol–gel process. A series of GSs/TiO$_2$ structures were investigated for the splitting of water under UV–Vis light in the mixture including sulfide/sulfite ions. A GSs/TiO$_2$ composite with 5 wt% graphene oxide (GO) showed a hydrogen generation rate of 8.6 μmol h^{-1} which is much higher than that of stand-alone TiO$_2$ crystal (4.5 μmol h^{-1}). The improved catalytic efficiency of GSs/TiO$_2$ was attributed to the good conductivity of GSs, which facilitates the motion of electrons to the surface of the photocatalyst. Moreover, the decreased performance of the composite with 10 wt% GO can be accounted for by the concurrence of electrons and holes, causing their recombination, which diminished the photocatalytic activity for water splitting. To innovate the material types, Kim et al. incorporated nanographene oxides (NGOs) with TiO$_2$ to create a core–shell structure of NGO/TiO$_2$ before it was photoreduced to form r-NGOT for photocatalytic water splitting (Kim et al., 2011). Besides, TiO$_2$ deposited on the μm-size r-GO (r-LGOT) was also fabricated to compare the catalytic efficiency (Fig. 5). Photocatalytic reactions were measured under UV irradiation with methanol as an electron donor. The results indicated that the r-NGOT core–shell showed the highest yield of hydrogen evolution with the amount of NGO of 0.7 wt%. The hydrogen production rate of the r-NGOT composite with a core–shell structure is faster than that of r-LGOT and bare TiO$_2$. This outcome can be attributed to the presence of r-GO, which impeded electron–hole pair reconsolidation and improved the moving of electron on the surface of r-NGOT. Moreover, the addition of platinum onto r-NGOT (Pt/r-NGOT) remarkably reinforced the catalytic activity for hydrogen evolution. Hydrogen was generated at a rate of 50 μmol h^{-1} for Pt/r-NGOT-0.7 and 27 μmol h^{-1} for Pt/TiO$_2$. The enhanced performance of hydrogen evolution was attributed to the good conductance of r-NGOT, which can boost the charge separation as well as the mobility of electron. In addition, r-NGOT created a convenient path for the motion of electrons from the TiO$_2$ CB to Pt sites.

To date, scientists have focused on the improvement of visible-light-driven photocatalysts to maximize the exploration of solar energy, because visible light is account for 53% of solar energy, whereas this percentage is only 4% for UV rays. As an attempt to improve the visible light absorption, Agegnehu et al. fabricated vanadium-doped TiO$_2$ NR on reduced graphene oxide through a facial hydrothermal method and the performance of obtained materials was investigated (Agegnehu et al., 2016). For intensive understanding, V-doped TiO$_2$ NPs with various proportions of vanadium, including 5, 10, and 15 wt% were coated on RGO to form nanocomposites. High-resolution TEM images of 10% V-doped TiO$_2$ and 10% V-doped TiO$_2$/RGO are shown in Fig. 6(a,b). The photocatalytic activity was evaluated under a 300 W xenon arc lamp as a light source for irradiation in a 20% aqueous methanol solution. The obtained result revealed that 10% V-doped TiO$_2$/RGO exhibited the highest performance, with a hydrogen generation rate of 120 μmol h^{-1}. In comparison, the speed of hydrogen formation of 10% V-doped TiO$_2$/RGO is four times quicker than that of 5% V-TiO$_2$, 1.6 times quicker than that of 10% V-TiO$_2$, and twice
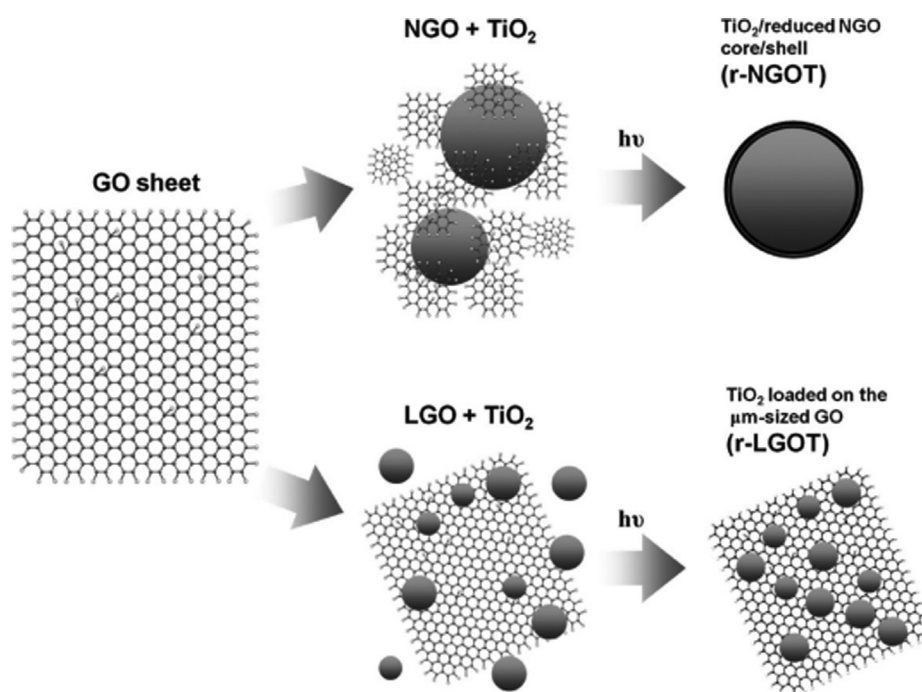
Fig. 5   Representation of the synthesis of r-NGOT and r-LGOT (Kim et al., 2011).
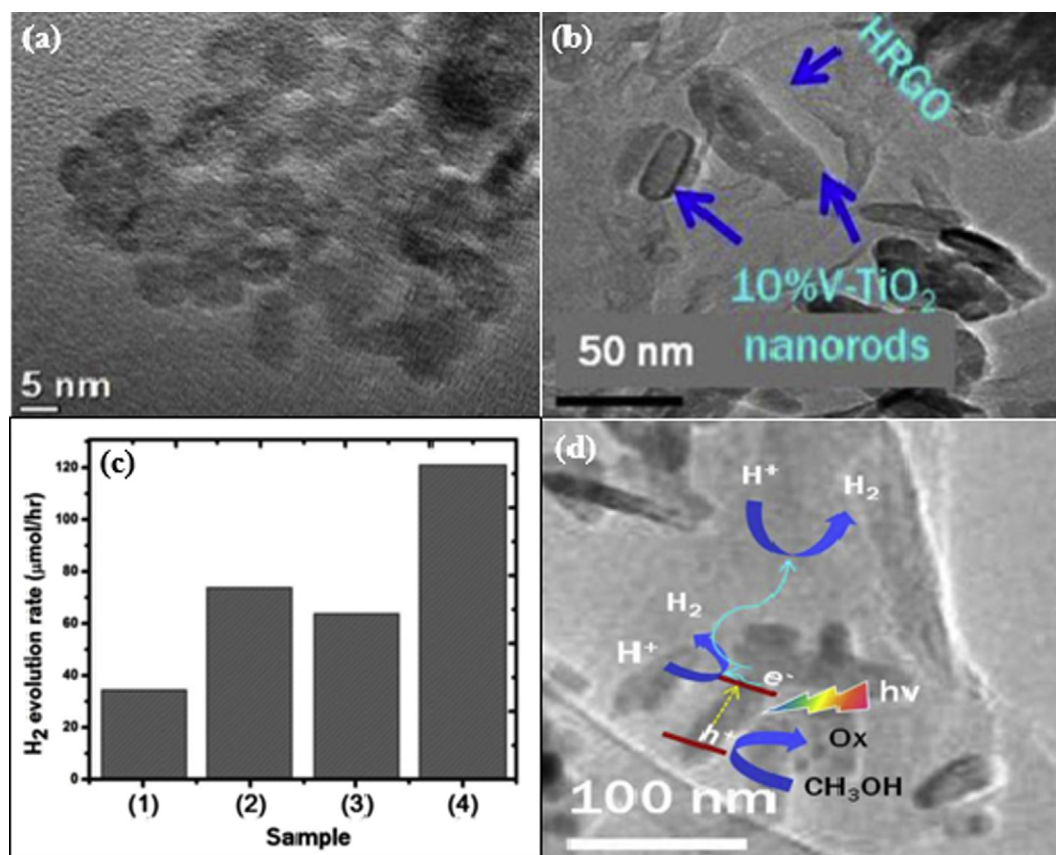
Fig. 6 (a) HRTEM image of 10%V-TiO$_2$ nanostructure. (b) TEM image of 10%V-TiO$_2$/RGO nanocomposite. (c) H$_2$ production rate under visible light irradiation: (1) 5%V-TiO$_2$, (2) 10%V-TiO$_2$, (3) 15%V-TiO$_2$, and (4) 10%V-TiO$_2$/RGO. (d) Schematic illustration of the photocatalytic reaction mechanism for 10%V-TiO$_2$/RGO (Agegnehu et al., 2016).

as fast as that of 10% V-TiO$_2$ (Fig. 6c). The highest hydrogen generation rate of 10% V-TiO$_2$/RGO in compare to the rest of the studied samples is attributed to two factors. First, the doping of vanadium onto TiO$_2$ reduced its bandgap width from 3.1 eV for bare TiO$_2$ to 2.51 eV, hence improving the light absorption. Second, RGO acts as a cocatalyst, which can trap the excited electrons, leading to suppress the charge recombination (Liu et al., 2010; Perera et al., 2012). Beside, RGO provides active sites for photoreduction reaction of water (Xiang et al., 2012). In the suggested reaction mechanism (Fig. 6d), the photocatalyst absorbs a photon from visible light illumination to separate the excitons. As a result, the negative electrons are promoted to the CB and the positive holes are located in the VB. These electrons can be moved to the surface of V-TiO$_2$ and the reduced graphene oxide sheets to facilitate the proton reduction reaction. This motion significant limits the recombination of charged particles, leading to improved photocatalytic performance for hydrogen evolution.

Recently, the simultaneous doping of metal ions and graphene for TiO$_2$ was a subject of continued research to enhance photocatalytic hydrogen production activity. Lang et al. fabricated an Ag-rGO-TiO$_2$ composite by depositing Ag nanocubes and TiO$_2$ nanolayers on the surface of reduced graphene oxides (Lang et al., 2018). Moreover, the authors also created Ag-TiO$_2$ for the comparison. Their structures are shown in Fig. 7(a,b). Catalytically, under visible light with methanol/water (20 vol% methanol), Ag-rGO-TiO$_2$ gave a hydrogen forma-

tion rate per mass unit of 0.53 μmol g^{-1} h^{-1}, whereas TiO$_2$ and Ag-TiO$_2$ were not found to be photocatalytically active. The enhanced activity was accredited to the performance of rGO as a conductive bridge for the transportation of electrons from Ag to TiO$_2$. In addition, the formation of a Schottky barrier on the surface of rGO-TiO$_2$ reinforces the hot electron pervasion from rGO to TiO$_2$, as shown in Fig. 7d. For the Ag-TiO$_2$ structure, the hot electrons recombine with holes owing to the lack of a formed barrier (Fig. 7c).

2.2.2.2. Transition metal dichalcogenides/TiO$_2$ composites. Another class of 2D materials is the TMDs, which are also considered as potential candidates for incorporation with graphene to boost the efficiency of TiO$_2$ materials in photocatalytic applications. For example, MoS$_2$/TiO$_2$ catalysts with various contents of MoS$_2$ were fabricated by Zhu's group through a facial mechanochemistry method (Zhu et al., 2015). These catalysts were evaluated in terms of their photoactive yield under UV irradiation. The results revealed that 4%-MoS$_2$/TiO$_2$ gave the greatest performance, with a reaction rate of 150.7 μmol h^{-1}, whereas pure TiO$_2$ only had a hydrogen generation rate of 3.1 μmol h^{-1}. The authors explained that MoS$_2$ acts as an electron container, which prevents the remix of electron–hole pairs. Moreover, the good conductivity of MoS$_2$ facilitates photo-induced charge separation, leading to improved catalytic performance. Ma and coworkers performed an interesting study by using a MOF as a reactant to
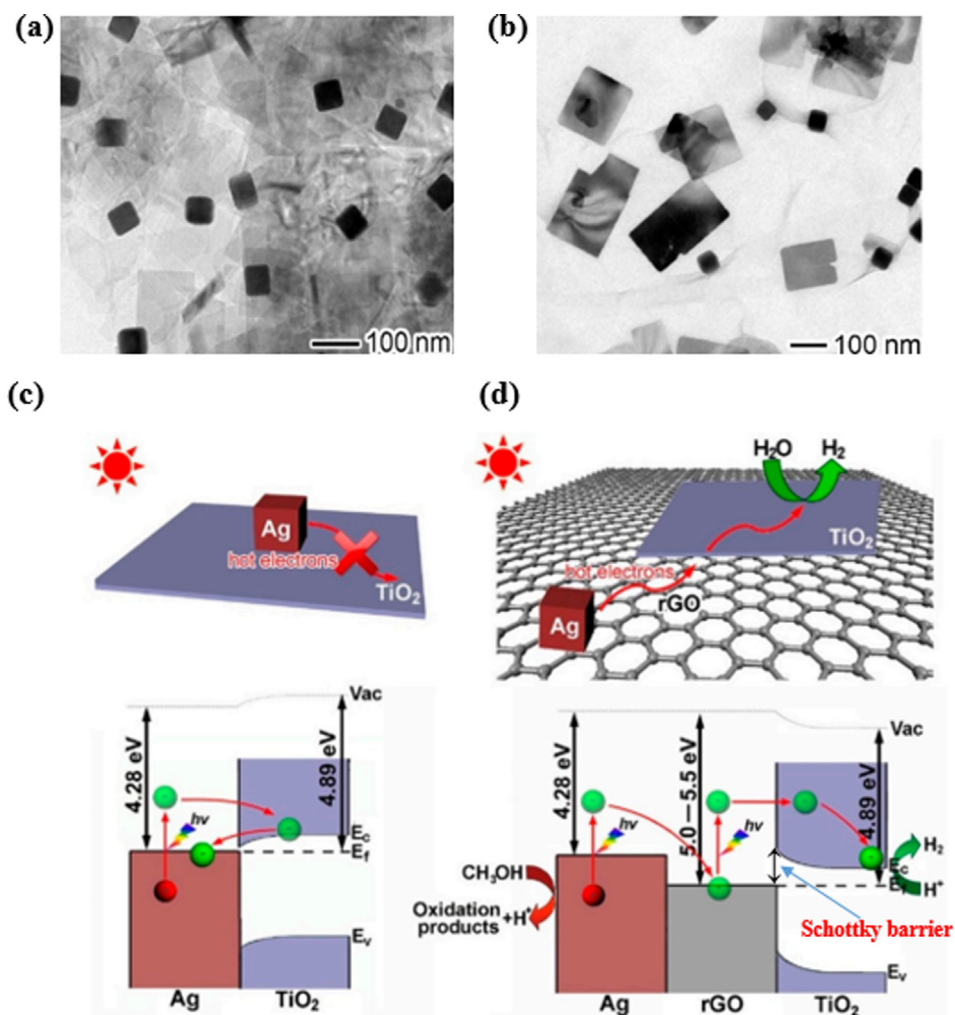
Fig. 7 (a) TEM image of Ag-TiO₂ hybrid structure. (b) TEM image of Ag-rGO-TiO₂ hybrid structure, and schematic representation of the photocatalytic reaction mechanism for Ag-TiO₂ (c) and Ag-rGO-TiO₂ (d) under visible light illumination (Lang et al., 2018).

fabricate a flower-like MoS_2/TiO_2 nanohybrid system through a facial hydrothermal process (Ma et al., 2016). An SEM image of MoS_2/TiO_2 is shown in Fig. 8a. Photocatalytic experiments were conducted in the visible light condition with fluorescein as a photosensitizer. A remarkable enhancement in the photocatalytic activity was recorded, showing a yield of hydrogen evolution rate per mass unit of 10046 $\mu mol\ h^{-1}\ g^{-1}$ (Fig. 8b). This performance was ascribed to the formation of active centers and uniform dispersion of the MoS_2 and TiO_2 phases, facilitating the motion of electrons to reduce protons. In the proposed mechanism, excited electrons from fluorescein move to the CB of TiO_2. Later, these electrons transfer to the surface of MoS_2 before facilitating the reduction of water (Fig. 8c). Jing et al. deposited WS_2 onto mesoporous TiO_2 (m-TiO_2) for the photocatalytic HER (Jing and Guo, 2007). The coating of WS_2 improved the light absorption ability of TiO_2, contributing to the enhancement in the yield of TiO_2. A hydrogen formation rate per mass unit of 2.2 $\mu mol\ h^{-1}\ g^{-1}$ was observed for WS_2/m-TiO_2 with Pt as a cocatalyst under visible light irradiation. Xiang et al. investigated the influence of MoS_2 and graphene as cocatalysts for the photocatalytic hydrogen generation of TiO_2 NPs (Xiang et al., 2012). TiO_2/MoS_2/graphene with the different amounts of

MoS_2 and graphene were prepared by a hydrothermal way. The structural properties were analyzed by TEM, as can be seen in (Fig. 9(a,b)). Photocatalytic experiments on these composites were carried out under UV irradiation with ethanol as a scavenger. A TiO_2/MoS_2/graphene composite with 0.5 wt% MoS_2/graphene (95/5 wt%) showed the highest activity, with a hydrogen generation rate of 165.3 $\mu mol\ h^{-1}$. Compared to the others, the hydrogen generation rate of TiO_2/MoS_2/graphene is four and five times higher than that of TiO_2/MoS_2 and TiO_2/graphene, respectively (Fig. 9c). This yield can be explained by the fact that the MoS_2/graphene mixture plays a pivotal key in the prevention of charge recombination, thanks to a synergetic effect, and supplies numerous active sites for the HER. The mechanism is illustrated in Fig. 9d.

2.2.2.3. Metal oxides/TiO₂ composite. Zinc oxide (ZnO) is widely studied in photocatalytic applications, owing to its high photochemical stability, photosensitivity, large bandgap, and nontoxicity. Thus, the incorporation of ZnO and TiO_2 has been studied for the field of photocatalysis. For example, Hussein et al. successfully synthesized ZnO/TiO_2 nanocomposites for the photocatalytic HER (Hussein et al., 2013). Catalytically, the activity of the catalysts was tested in a methanol
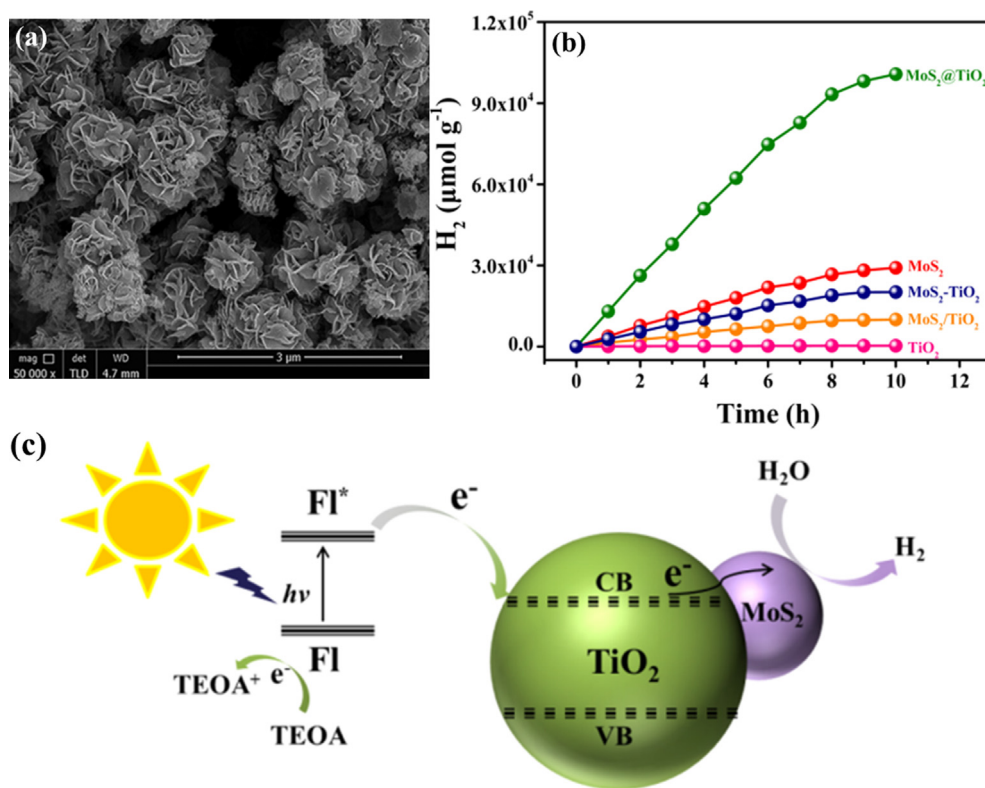
Fig. 8 (a) SEM image of MoS$_2$@TiO$_2$ hybrid. (b) H$_2$ produced by various catalysts in a mixture containing acetone and TEOA, and fluorescein over 10 h. (c) Schematic representation of the photocatalytic reaction mechanism for MoS$_2$@TiO$_2$ under visible light (Ma et al., 2016).

solution under UV–Vis irradiation. This nanocomposite demonstrated increased HER performance compared to that of the stand-alone TiO$_2$. The observed increased activity of this nanocomposite was ascribed to the larger surface area and total pore volume, and smaller interface resistance. Another study on ZnO/TiO$_2$ was reported by Xie and coworkers (Xie et al., 2017). The authors mixed TiO$_2$ and ZnO with different ratios before depositing Pt as a cocatalyst for hydrogen evolution. The results revealed that 0.5 wt% Pt/TiO$_2$-ZnO gave the best performance, with a hydrogen generation rate per mass unit of 2150 μmol h^{-1} g^{-1} under visible light irradiation. Considering the homogeneous catalysts, the hydrogen generation rates per mass unit are 68 and 3.0 μmol h^{-1} g^{-1} for TiO$_2$ and ZnO, respectively. Furthermore, the durability of the catalyst was also tested for H$_2$ production. The productivity reduced by only 12% and 23% compared with the first test time after 7 and 14 days, respectively.

One promising approach to fabricating metal oxide/TiO$_2$ composites is to use MOFs as precursors. The advent of MOFs opened a new chapter in the field of materials science and technology (Low et al., 2014). MOFs are known as the first member in the family of cage-like porous materials, which are constructed by the combination of metal clusters and organic compounds (Lu et al., 2014). Traditionally, MOFs were used in gas separation, gas storage, catalysis, sensors, and drug delivery applications, thanks to their outstanding properties such as large surface area, high porosity, and adjustable chemical structures (Chaemchuen et al., 2013). Furthermore, MOFs were used as sacrificial templates to create metal oxide/TiO$_2$

hybrids for the photocatalytic HER. Several illustrative metal oxide/TiO$_2$ systems based on MOF materials are discussed herein. Bala and coworkers utilized a Co-based MOF as a precursor to synthesize Co$_3$O$_4$/TiO$_2$ nanocomposites for photocatalytic splitting water (Bala et al., 2015). This material with 2 wt% displayed a reaction rate of 7 mmol g^{-1}h^{-1} under UV illumination. The intensified catalytic performance was attributed to the formation of a homogeneous catalyst and the presence of Co$_3$O$_4$ as a co-catalyst to boost the electron transfer as well as electron–hole pair separation. In a similar example, Mondal and Pal used a Cu-based MOF as a sacrificial template to fabricate composites (Mondal and Pal, 2016). The optimized Cu/CuO/TiO$_2$ hybrid nanocomposite gave a yield of 286 mmol g^{-1}h^{-1} under solar illumination, which was much better than that of a conventional CuO/TiO$_2$ hybrid system, owing to the formation of a small heterojunction and Cu loading into the TiO$_2$ matrix. Dekrafft et al. utilized an Fe-based MOF to fabricate an Fe$_2$O$_3$@TiO$_2$ core–shell structure before depositing Pt on the surface for the photocatalytic HER, as shown in Fig. 10a (Dekrafft et al., 2012). The catalyst exhibited a much faster hydrogen formation rate than those of Fe$_2$O$_3$, TiO$_2$, and their mixture. The plot of hydrogen evolution with respect to time is illustrated in the inset of Fig. 10b.

2.2.2.4. Transition metal carbide/TiO$_2$ composites. Transition metal carbides are an important member of the young family of MXenes. They have gained much attention for potential applications, owing to their outstanding thermal, optical,
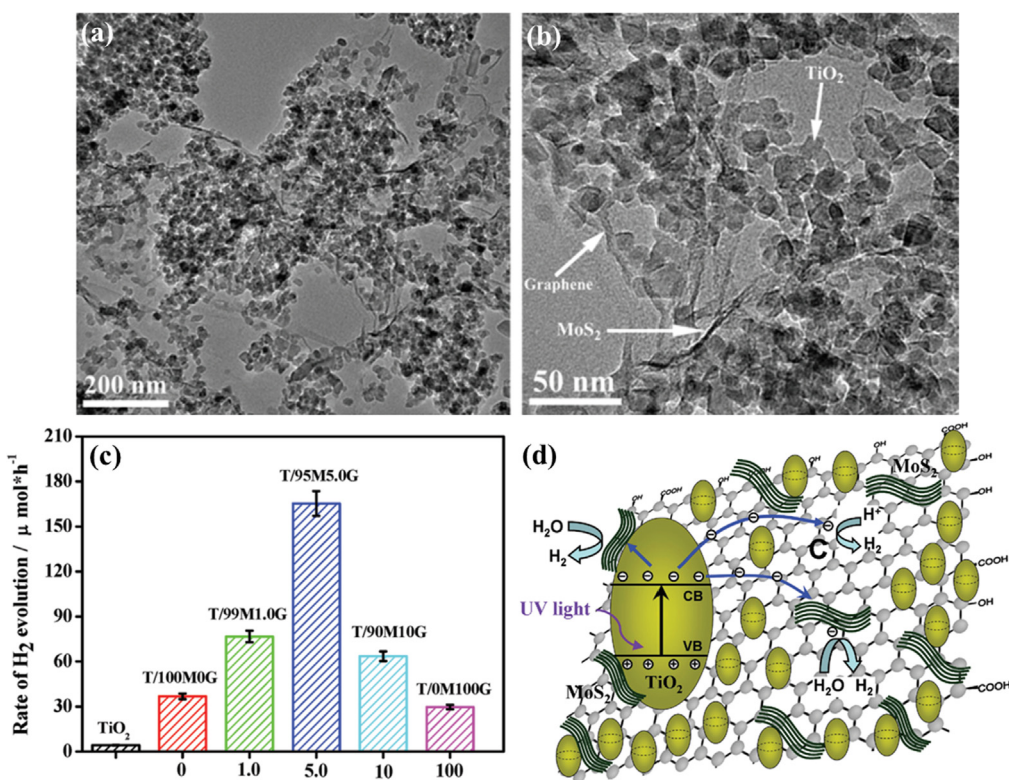
Fig. 9 (a,b) TEM image of TiO$_2$/95 M5.0G hybrid structure. (c) Comparison of H$_2$ evolution rate by various catalysts. (d) Schematic representation of the photocatalytic reaction mechanism for the TiO$_2$/MoS$_2$/graphene system under visible light illumination (Xiang et al., 2012).
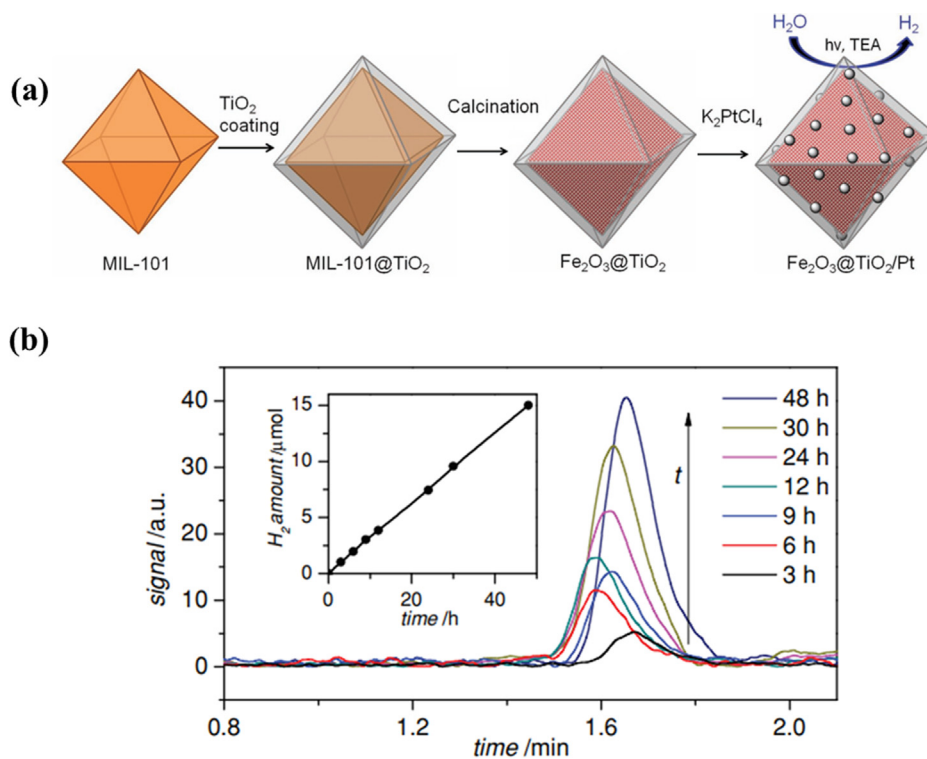
Fig. 10 (a) Representation for the synthesis of Fe$_2$O$_3$@TiO$_2$ by coating TiO$_2$ onto the surface of MIL-101, followed by calcination, and its use for photocatalytic H$_2$ generation after the addition of Pt particles. (b) H$_2$ created by Fe$_2$O$_3$@TiO$_2$ in 20/1 v/v H$_2$O/TEA for different times, with a 420 nm filter. The inset shows the amount of H$_2$ generated over this time period (Dekrafft et al., 2012).

mechanical, and electronic features (Anasori et al., 2017; Hantanasirisakul and Gogotsi, 2018; Pang et al., 2019). Therefore, the combination of metal carbides and TiO$_2$ has been explored for catalytic utilization in energy conversion. In 2016, a mixture of metal carbide/TiO$_2$ was first reported by the Wang group for the separation of water into hydrogen under visible light (Wang et al., 2016). TiO$_2$/Ti$_3$C$_2$T$_x$ composites were investigated with respect to their photocatalytic activity with different ratios. The optimal sample is TiO$_2$/Ti$_3$C$_2$T$_x$-5%, exhibiting a hydrogen generation rate per mass unit of 17.8 µmol h^{-1} g^{-1} upon visible light irradiation, which is superior to that for the homogeneous catalysts under the same condition. The reason for this is that the Ti$_3$C$_2$T$_x$ can facilitate the electron-hole separation and charge transportation, thus, promoting the overall performance of photocatalytic HER. Recently, Peng et al. provided a new approach to fabricate metal carbide composites for photocatalytic applications (Peng et al., 2018). Briefly, TiO$_2$ nanolayers were grown on Ti$_3$C$_2$T$_x$ by a hydrothermal method before undergoing photodecomposition of copper metal to form Cu$_y$/TiO$_2$@Ti$_3$C$_2$T$_x$. Catalytic reactions proceeded under simulated solar light in methanol solution. Hydrogen was generated at a hydrogen production rate of 860 µmol h^{-1} for one gram Cu/TiO$_2$@Ti$_3$C$_2$T$_x$ catalyst. In comparison, 1 g TiO$_2$@Ti$_3$C$_2$T$_x$ catalyst had a slow hydrogen production rate of only 65 µmol h^{-1}. This result was ascribed the presence of Cu species as a cocatalyst and Ti$_3$C$_2$T$_x$ acting as an assistant of TiO$_2$ for removing holes, thereby facilitating detaching the excitons and electron transfer. From the initial results, metal carbide/TiO$_2$ composites have opened a promising horizon for scientists to find the ideal catalysts for hydrogen production from water splitting.

2.2.3. Doping
2.2.3.1. Metal-doped TiO$_2$.
Modifying TiO$_2$ with other heteroatoms can change its bandgap width as well as extend the optical adsorption range, leading to enhanced photocatalytic activity. Noble metals such as Pt, Pd, Ru, Rh, Au, and Ag are considered the most effective materials for the field of

catalysis in general and the photocatalytic HER in particular (Banerjee et al., 2015; Huang et al., 2018; Ouyang et al., 2018; Wu et al., 2013a,b; Wu et al., 2016a,b; Zhang et al., 2016). However, the important issue is that their price is high. The use of a small amount of precious metals to improve the catalytic activity of TiO$_2$ is an alternative approach. For instance, Zhu et al. deposited Pt onto a circular template of C-HS-TiO$_2$ created from D-glucose as a precursor (as shown in Fig. 11a) (Zhu et al., 2016). The results indicated that 1 wt% Pt/C-HS-TiO$_2$ gave the highest hydrogen production rate of 2856.8 µmol h^{-1} compared with economic TiO$_2$ and C-TiO$_2$ hollow sphere (Fig. 11b). The reason for this that the addition of Pt onto C-HS-TiO$_2$ with the hollow spherical morphology improved the optical absorption ability in the visible light region. Moreover, a stability test of the photocatalysts was conducted after 22 days. The yield only declined by a small percentage of 8% for 1 wt% Pt/C-HS-TiO$_2$ (Fig. 11c). Another platinized TiO$_2$ was reported by Li et al. (2015a,b). The authors fabricated sub-10-nm rutile TiO$_2$ NPs by a facile hydrolysis method before doping 1 wt % Pt into these particles as a cocatalyst. The photocatalytic system was tested under the different light sources in 10 ml methyl alcohol (sacrificial reagent). A reaction rate per mass unit of 1954 µmol h^{-1} g^{-1} was observed under simulated solar light, whereas the hydrogen rate per mass unit observed with visible light proving energy for the photocatalytic reaction was 932 µmol h^{-1} g^{-1}. These results were confirmed by the appearance of OH- groups on the surface of TiO$_2$, which contribute to decreasing its bandgap. Additionally, TiO$_2$ with small particle sizes increases the proportion of surface/sub-surface deficiencies to overcome the adverse effects of the bulk phase, leading to improved electron–hole separation. To date, the highest quantum efficiency is attributed to Pt-doped TiO$_2$, which was reported by Guayaquil-Sosa et al. (2017). Mesoporous TiO$_2$ with special properties as mentioned above is modified with various amounts of Pt, including 1.00, 2.50, and 5.00 wt%. Among these, 2.5 wt% Pt-TiO$_2$ exhibited the highest quantum yield of
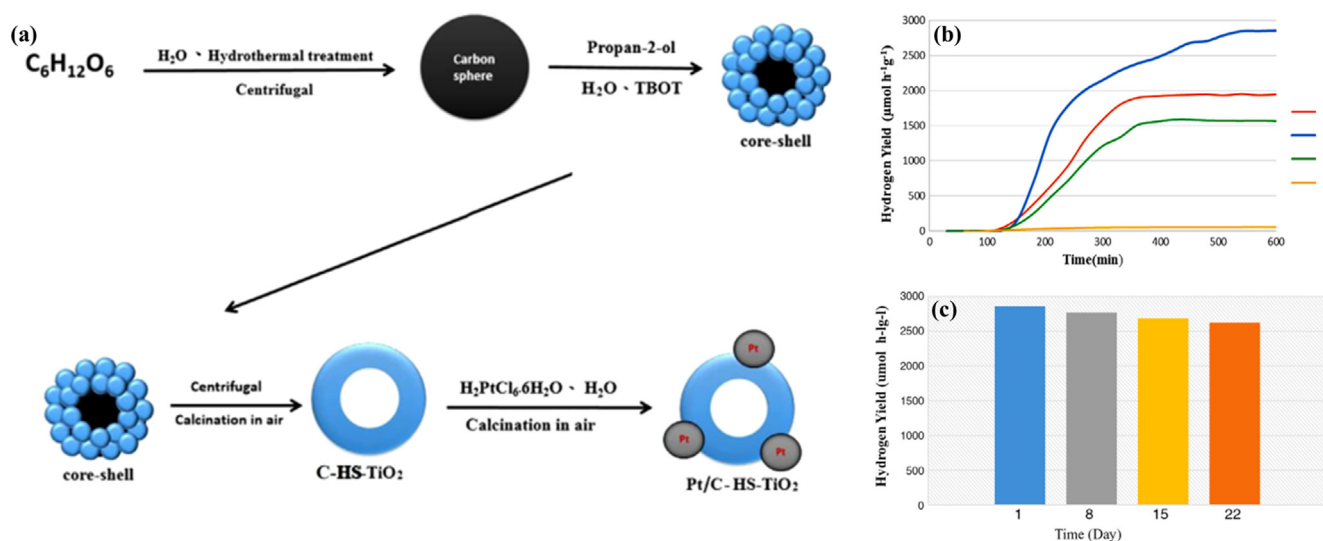
Fig. 11 (a) Schematic diagram of the preparation of Pt/C-HS-TiO$_2$. (b) H$_2$ produced by different catalysts under visible light irradiation: (x) 0.5 wt% Pt/C-HS-TiO$_2$, (y) 1.0 wt% Pt/C-HS-TiO$_2$, (z) 1.5 wt% Pt/C-HS-TiO$_2$, (t) 2.0 wt% Pt/C-HS-TiO$_2$. (c) Recycling of 1.0 wt% Pt/C-HS-TiO$_2$ for photocatalytic hydrogen production at room temperature (Zhu et al., 2016).

22.6% due to the effective reduction of the optical bandgap from 2.99 eV (bare TiO_2) to 2.34 eV.

Apart from Pt, Au has also drawn significant attention as a dopant for improving the performance of TiO_2 as a photocatalyst for the HER. Au is commonly fabricated as nanoscale structures, such as NPs, NRs, nanowires to incorporate the other materials for the catalytic reaction. Several studies indicated that Au with a particle size of less than 5 nm exhibits high catalytic performance (Haruta 1997; Valden et al., 1998). For example, Fang et al. generated a mesoporous Au-TiO_2 nanocomposite through a copolymer-assisted sol–gel method for solar hydrogen evolution (Fang et al., 2012). The results revealed that in the presence of ascorbic acid, water is reduced to hydrogen at a rate per mass unit of 7 µmol h^{-1} g^{-1} under visible light, which is 3-fold higher than that for Pt-TiO_2 under similar experimental conditions. Three reasons were suggested to explain these results. The catalytic activity of Au-TiO_2 was attributed to the contribution of defect/impurity states and the poorly visible light absorption of the TiO_2 matrix was improved by the Au surface plasmons. Moreover, the Au NP plays an important role in providing electrons to TiO_2 for photoreduction. Another special structure of Au investigated for its photocatalytic activity for the HER is Au NRs (AuNRs). Wu et al. created AuNR/TiO_2 nanodumbells as a potential candidate for the photocatalytic HER by coating TiO_2 on the two ends of gold NRs through a wet-chemical method (Fig. 12a) (Wu et al., 2016a,b). The photocatalytic performance of these catalysts is displayed in Fig. 12b. Specifically, AuNR/TiO_2 nanodumbells exhibited a yield of 11.6 µmol g^{-1}h^{-1} upon visible light irradiation, whereas the AuNR@TiO_2 core–shell structure did not show any catalytic activity under similar experimental conditions. These results can be justified by the fact that the transfer of hot electrons

takes place in the photoreduction of water for AuNR/TiO_2 nanodumbells (Fig. 12c). The AuNR@TiO_2 core–shell structure only exhibits plasmon-induced resonance energy transfer (Fig. 12d). The third noble metal that has been applied for catalytic utilization is silver (Ag). Liu et al. synthesized a TiO_2 nanosheet film (TiO_2-NSF) by a simple hydrothermal process before depositing Ag NPs on its surface (Liu et al., 2014a,b). Under the irradiation of UV–Vis light, the Ag/TiO_2-NSF was found to be 8.5 times more effective than the homogeneous TiO_2 catalyst. The reason for this is that the Ag NPs support the prevention of the remix of electron–hole pairs, leading to enhanced electron transfer in the reduction of water. The second reason is the synergetic effect between the electron transfer and surface plasmon resonance absorption. The codoping of noble metals on TiO_2 has also been researched for photocatalytic H_2 production from water. Rahul et al. incorporated Au-Pt NPs and Ti^{3+} to generate an Au-Pt/Ti^{3+} nc-TiO_2 catalyst before it was reconstituted into titania inverse opal (Au-Pt/Ti^{3+} io-TiO_2) for solar water splitting (Rahul et al., 2018). Hydrogen was detected at a rate per mass unit of 181.77 mmol h^{-1} g^{-1} for the Au-Pt/Ti^{3+} io-TiO_2 photocatalyst, which is higher than any other catalyst, including Au-Pt/Ti^{3+} nc-TiO_2, Au/Ti^{3+} nc-TiO_2, and Pt/Ti^{3+} nc-TiO_2. This activity is attributed to the appropriate photonic effects on TiO_2 electronic absorption properties. Another pair of noble metals was used to produce Ag-Au bimetallic cluster-doped TiO_2. This incorporation enhanced the light adsorption region from 400 to 650 nm (Patra and Gopinath, 2016). As a result, the Ag-Au/TiO_2 composite displayed a hydrogen production rate per mass unit of 718 mmol h^{-1} g^{-1}, whereas the rate was much lower for the Ag-TiO_2 and Au-TiO_2 mixtures. The improved catalytic activity is mainly attributed to the formation of a Schottky junction. Moreover, the generation of hot electrons also has a significant function in boosting the reaction rate. A fascinating study utilizing MOFs as a precursor to synthesize TiO_2 was reported by Yan et al. (2017). NH$_2$-MIL-125(Ti) was pyrolyzed at 400 °C to form hierarchical TiO_2 before different amounts of Pd were deposited on it for the photocatalytic HER (Fig. 13a). Pd/TiO_2 with 1.5 wt% showed excellent performance of 979.7 µmol h^{-1} under UV–Vis irradiation, whereas this value was 112.7 µmol h^{-1} under simulated solar light (Fig. 13b,c). These yields were attributed to the positive synergetic effect, constituting convenient conditions for the splitting and conveyance of electron–hole pairs.

Non-noble metals are also utilized to intensify the photocatalytic activity of TiO_2 (Dholam et al., 2009; Sadanandam et al., 2013). Many studies have demonstrated that copper metal has special property to catalyze certain reactions in the area of energy conversion, such as the CO_2 reduction reaction (Maina et al., 2017). Hence, the combination of copper and TiO_2 materials can provide promising candidates for hydrogen evolution with a high yield. For example, Cu-deposited TiO_2 for the photocatalytic HER was first reported by Wu et al. (Wu and Lee, 2004). The optimal sample with 1.2 wt% Cu showed a reaction rate 10 times faster than that with bare titania. The oxidation of Cu was observed during the photoreduction process. This work represented an initial step in using Cu to boost the catalytic activity of TiO_2. In 2017, Rather et al. generated a Cu^{+1}/Cu^0-TiO_2 mesoporous nanocomposite (Cu-mpTiO_2) for solar hydrogen production (Rather et al., 2017). Cu-mpTiO_2 photocatalysts were created from mesoporous TiO_2 with high surface area and Cu NPs via incipient
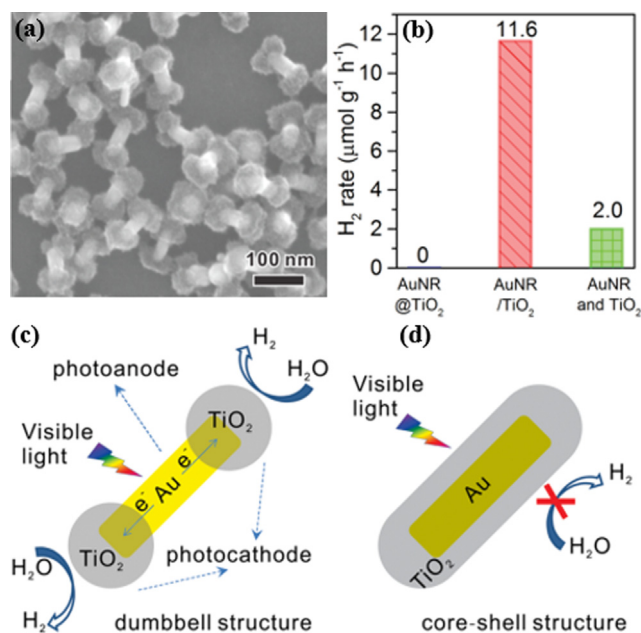
Fig. 12 (a) SEM image of the as-prepared AuNR/TiO_2 nanodumbells. (b) Photocatalytic hydrogen production rate of various catalysts. (c,d) Schematic representation of the photocatalytic reaction mechanism for (c) AuNR/TiO_2 dumbbell and (d) core–shell AuNR@TiO_2 under visible light (Wu et al., 2016).
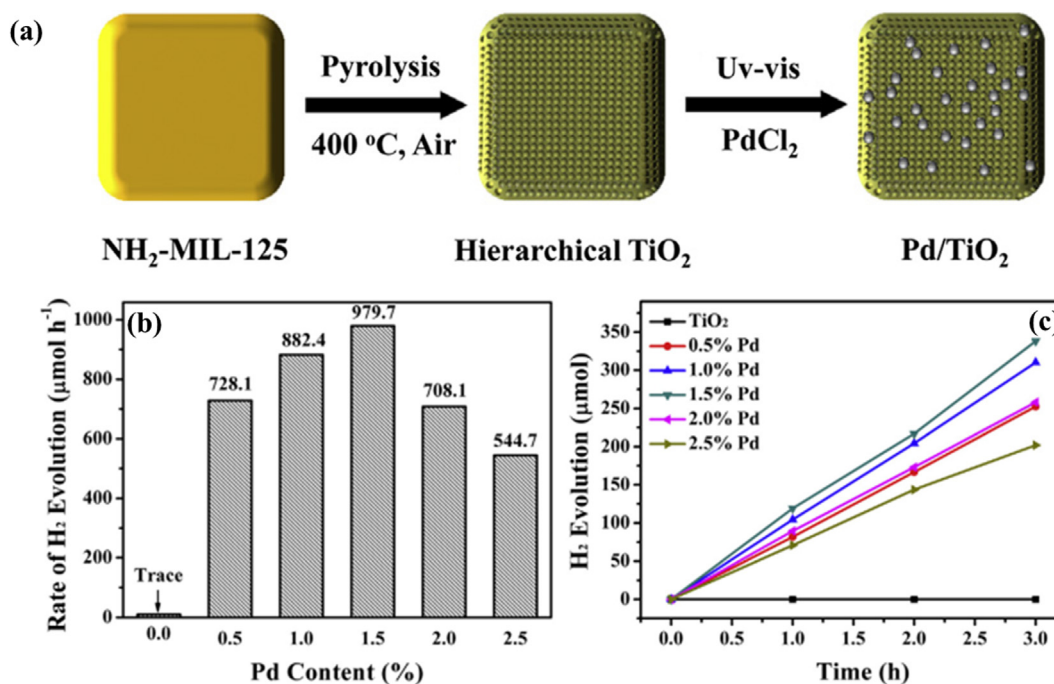
Fig. 13 (a) Representation of the fabrication of Pd/TiO$_2$ from NH$_2$-MIL-125. (b,c) H$_2$ produced by Pd/TiO$_2$ in 20 vol% methanol solution with different contents of Pd under UV–Vis light (b) and simulated solar light (c) (Yan et al., 2017).

wetness impregnation. The photoreactions were tested under direct sunlight in 20% vol. methanol. Water was photoreduced to hydrogen with an amount of 1000 μmol and an apparent quantum yield of 11.39%. In comparison, the apparent quantum efficiency of commercial Cu-TiO$_2$ is 4.1%, whereas the bare mesoporous TiO$_2$ did not show any performance. Recently, Montoya et al. synthesized various catalysts by depositing transition metals, including Ni, Co, and Cu, on the surface of TiO$_2$ to realize an improved photocatalytic hydrogen generation by a photoreduction method (Montoya and Gillan, 2018). All the transition metals used to modify TiO$_2$ resulted in higher performance than that of unmodified TiO$_2$. The best yield was observed for Cu(1%):TiO$_2$, with a hydrogen generation rate per mass unit of 8500 μmol h^{-1} g^{-1}. This was attributed to the function of the 3d transition metal, restraining the reformation of excitons and facilitating the transportation of electrons for the reduction of water.

Similar to noble metal-doped TiO$_2$, the codoping of TiO$_2$ with non-noble metals has also been studied for the HER (Luna et al., 2017; Sun et al., 2012, 2015). An example is Fe-Ni-codoped TiO$_2$ to achieve boosted visible-light-driven photocatalytic activity. Sun et al. investigated the catalytic activity of bare TiO$_2$, Ni-doped TiO$_2$, Fe-doped TiO$_2$, and Fe-Ni-codoped TiO$_2$ for water splitting under visible light (Sun et al., 2012). These catalysts were fabricated by an alcohol-thermal method. Based on the Brunauer–Emmett–Teller (BET) measurement, a relatively high surface area of 98.35 m^2 g^{-1} was estimated for Fe-Ni/TiO$_2$ (5 wt% Fe and 4.0 wt% Ni), which is approximately 2-fold larger than that of bare TiO$_2$. As a result, this catalyst displayed a hydrogen evolution rate of 361.64 μmol g^{-1} h^{-1} in the ethanol solution, whereas Fe-TiO$_2$ and Ni-TiO$_2$ had a lower rate, and TiO$_2$ alone was not active under similar conditions. The reason for this is that the co-doping of Fe and Ni improved the visible

light absorption capacity of TiO$_2$, which was verified by UV–Vis spectroscopy. Also, the enhanced separation of electron–hole pairs was proved through photoluminescence spectroscopy. The reaction mechanism is shown in Fig. 14 A similar example is Ni-Pd/TiO$_2$, which was reported by Luna et al. (Luna et al., 2017). Ni-Pd/TiO$_2$ was created in a solution of ammonium hydroxide via a radiolysis method. Single metal-doped TiO$_2$ was fabricated for comparison. Photocatalytic experiments were performed under a 400 W mercury arc as a UV–Vis illumination source. In methanol solution (50% vol.), hydrogen was generated with a production rate of 200 μmol h^{-1}. The bimetallic doping created a synergetic effect in facilitating electron transfer. Moreover, Ni-Pd NPs play a vital role as catalytic centers for the formation of hydrogen.
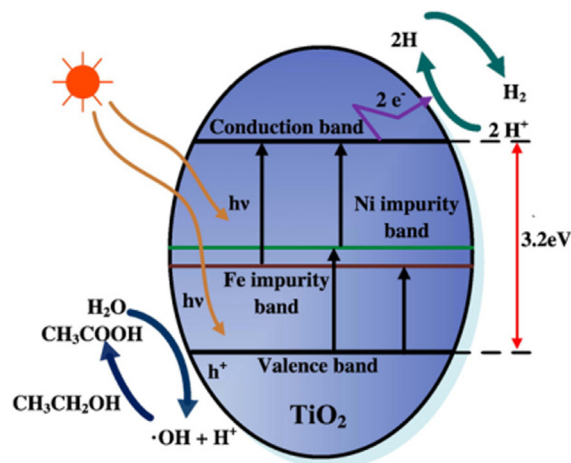
Fig. 14 Schematic illustration of solar water splitting for Fe-Ni/TiO$_2$ under visible light illumination (Sun et al., 2012).

Additionally, co-metal doping has also been utilized to boost the catalytic activity of TiO_2. For example, Tanigawa et al. synthesized Cr/Ta co-doped anatase TiO_2 (Cr,Ta-TiO_2(A)) and rutile TiO_2 (Cr,Ta-TiO_2(R)) for hydrogen production by a facile hydrothermal method (Tanigawa and Irie, 2016). Platinum was then deposited onto these materials for water splitting applications. The photocatalytic experiments were implemented under visible light illumination. The HER takes place in the presence of I^- for Cr,Ta-TiO_2(A) with a hydrogen evolution rate per mass unit of 11.7 µmol h^{-1} g^{-1}, whereas oxygen evolution only occurs in the presence of IO_3^- for (Cr,Ta-TiO_2(R)). This result could be explained by the fact that the Cr 3d orbital in Cr,Ta-TiO_2(A) was accounted for the oxidation iodide ion, and was not concerned in O_2 evolution, whereas the electrons in the CB of Cr,Ta-TiO_2(A) were accounted for the HER.

2.2.3.2. Nonmetal-doped TiO_2. Many studies have demonstrated that N-doped TiO_2 not only decreases the bandgap width of TiO_2, but also improves the photocatalytic performance for the HER (Hou et al., 2017; Khore et al., 2017; Liu et al., 2016; Preethi et al., 2016; Reddy et al., 2017; Taherinia et al., 2019). For instance, the Sonawane group researched the yield of N-doped TiO_2 for the photocatalytic HER (Khore et al., 2017). They found that N-TiO_2 had a high hydrogen generation rate per mass unit of 7990 µmol h^{-1} g^{-1} under natural sunlight. Moreover, the catalytic activity of N-TiO_2 was tested under a xenon lamp, and the hydrogen generation was detected with a rate per mass unit of 4740 µmol h^{-1} g^{-1}. These results were explained by the fact that natural sunlight includes both UV and visible light, and narrowed bandgap width is due to the appearance of nitrogen in the TiO_2 lattice via the Fourier transform infrared spectrum. Liu and coworkers prepared ultrafine N-doped TiO_2 through a simple solvothermal route with polyvinylpyrrolidone (PVP) as a nitrogen source (Liu et al., 2016). They observed that the photocatalyst with 0.1 g exhibited a significantly increased hydrogen generation rate per mass unit of 323 µmol h^{-1} g^{-1}, which is much quicker than that of TiO_2. The authors suspected that the boosted performance was related to the ultrafine particle size, the hydroxyl groups, and the addition of nitrogen on TiO_2. Hou and coworkers synthesized N-doped TiO_2 mesoporous nanofibers for the HER (Hou et al., 2017). They found that the nitrogenation of TiO_2 could improve the performance for the splitting of H_2O into hydrogen compared to the bare TiO_2. N-doped TiO_2 mesoporous nanofibers gave a hydrogen production rate per mass unit of 39.5 µmol h^{-1} g^{-1}, whereas the rate for the bare TiO_2 was 1.5 µmol h^{-1} g^{-1}. This high hydrogen production yield can be accounted for the narrow bandgap of N-doped TiO_2. The second nonmetal used as a dopant for TiO_2 is sulfur. Yang et al. successfully synthesized S-doped core–shell black TiO_2 for improved H_2 generation (Yang et al., 2013). This catalyst yielded a hydrogen production rate per mass unit of 0.258 mmol h^{-1} g^{-1}. The excellent performance was ascribed to the high amounts of Ti^{3+} and S in the shell layer, which broaden the optical absorption ability from UV light into the visible and near-infrared regions. Sun et al. mixed sulfur powder and TiO_2 nanotubes with an equal ratio to prepare Si-doped TiO_2 nanotubes (Sun et al., 2017). The photocatalytic performance was estimated under visible light in a methanol solution (20% vol.). The results

indicated that an excellent yield of hydrogen production rate per mass unit of 9610 µmol h^{-1} g^{-1} was attained, which was ascribed the presence of S_2^{2-} anions in the TiO_2 nanotubes. Moreover, the third group in used for improving the photocatalytic activity of TiO_2 is that of halogen elements such as Cl, Br, and F. Several works have revealed that these elements could broaden the optical absorption, leading to improvements in the photocatalytic HER (Gao et al., 2019, Luo et al., 2004, Yang et al., 2018). Recently, Andoshe et al. conducted a fascinating study by co-doing of nonmetal N and S to the TiO_2 NRs structure with the various contents for application as photoanodes for photoelectrocatalytic water oxidation (Andoshe et al., 2018). In this work, they increased the photocurrent density from 0.7 mA cm^{-2} (bare TiO_2 NRs) to 2.82 mA cm^{-2} ((N, S) co-doped TiO_2 NRs) at a potential of 1.23 V vs. RHE. The improvement in device performance was postulated to come from the newly created defect energy level near the valance band edge, which reduced the bandgap of TiO_2 from 3.1 eV to 2.88 eV. Notably, (N, S) co-doped TiO_2 NRs exhibited an external quantum efficiency of 97%, which is substantially higher than that of pristine TiO_2 NRs (19.1%) under UV light.

Another approach for increasing the catalytic activity of TiO_2 is simultaneous metal and nonmetal doping. For example, a systematic study of the modification of TiO_2 with cations and anions was conducted by Lin and Shih (2016). The authors fabricated a series of M/N-TiO_2 (M: Cr, Cu, Ni, Nb) structures by a microwave-supported hydrothermal process for solar hydrogen evolution. The photoreduction of water takes place in the presence of methanol as an electron donor under various light sources. The results revealed that Cu/N-TiO_2 exhibited the highest hydrogen production rate per mass unit of 27.4 µmol h^{-1} g^{-1} under UV light and 283 µmol h^{-1} g^{-1} under visible light. The synergistic effect created by copper and nitrogen doping can account for these outcomes. Zhang et al. investigated Cu/S-TiO_2 for catalyzing of the water-splitting process under visible light (Zhang et al., 2015a,b). Cu/S-TiO_2 showed enhanced catalytic activity in a methanol solution as an electron donor. Hydrogen was produced at a rate per mass unit of 7.5 mmol h^{-1} g^{-1}. In comparison, this quantity of S-TiO_2 was only 0.7 mmol h^{-1} g^{-1}, whereas hydrogen was not detected for bare TiO_2. The enhanced performance was attributed to the good dispersion of Cu species in S-TiO_2, creating a convenient condition for the separation and transportation of electrons in the photoreduction of water. In 2018, Mandari et al. used the rare earth metal Ga incorporated with N for doping TiO_2 in solar hydrogen production (Mandari et al., 2018). Ga/N-TiO_2 with 2% Ga displayed a reaction rate of 5.32 µmol h^{-1} which was attributed to the improvement in the optical absorption and efficient electron–hole pair separation.

Another study using the four elements Cu, Ga, In, and S to improve the photocatalytic ability of TiO_2 for the HER was reported by Kandiel and Takanabe (2016). Cu-Ga-In-S/TiO2 was fabricated by a solvent-induced deposition method. Copper–gallium–indium–sulfide (CGIS) with different weight percentages, including 1, 5, 10, 25, 50, and 75 wt%, was coated onto the surface of TiO_2 in toluene. Photocatalytic reactions were carried out under visible light with a mixture including catalyst and Na_2S/Na_2SO_3. Ru was used as a cocatalyst in a photoreactor system. The catalyst that showed the highest

yield was $CuGa_2In_3S_8$ (50 wt%)/TiO_2, which gave a hydrogen evolution rate of 50.6 μmol h^{-1}. The intensified activity was attributed to the extended visible light adsorption range of TiO_2 by CGIS. TiO_2 was not active in photocatalytic hydrogen evolution under visible light. Moreover, a small amount of CGIS also improved the photocatalytic activity of TiO_2. This could enable increased economic efficiency for large-scale applications.

3. Challenges and perspectives

TiO_2 photocatalysts are considered as promising materials for hydrogen production from photocatalytic HER. Many works have demonstrated that TiO_2-based photocatalysts exhibited excellent performance. Nevertheless, the main challenge of TiO_2 is its wide bandgap, which leads to rapid quenching of photo-induced excitons. This reduces the photocatalytic activity of TiO_2. Moreover, the effect of the synthetic methods on catalytic activity obviously needs to be investigated, and the electron transfer is also not clear. Although the reported TiO_2 materials showed high activity, the recycling of TiO_2-based photocatalysts has not been studied to save the cost of manufacturing in industrial applications. Furthermore, the investigation on mesoporous TiO_2 with high porosity and well-defined pore channels that facilitate the transportation of protons to catalytic centers needs more attention. In addition, the incorporation of two-dimensional materials (e.g., graphene, TMDs), MOF materials, and TiO_2 can also create promising candidates for solar hydrogen production. Finally, owing to the increasing development of computational methods, the properties of TiO_2-based catalysts such as the electronic density of states, band structures, and active sites can be thoroughly studied and designed toward high-performance photocatalytic HER. Thus, to achieve a better understanding and improved development of TiO_2 photocatalysis for the HER, a combination of empirical and theoretical study is required

4. Conclusion

In this review, the application of TiO_2-based catalysts in the reduction of water through photocatalysis has been discussed. Compared to other catalysts, TiO_2 has outstanding properties like low cost, high firmness, nontoxicity, and environmental friendliness. However, TiO_2 also has several disadvantages in photocatalytic applications, including a large bandgap, high hydrogen overpotential, and the remix of exciton. To tackle these problems, the different strategies involving metal deposition, nonmetal doping, graphene/TiO_2 hybrids, and MOF/TiO_2 composites have been applied to boost the catalytic activity of TiO_2. Moreover, the morphology and particle size also have a vital role in the extent of their photocatalytic characteristics. Therefore, a combination of compositional and structural engineering of TiO_2-based catalysts is expected to give better device performance. However, it needs more investigation in the near future.

Declaration of Competing Interest

The authors declare no conflicts of interest.

References

Agegnehu, A.K., Pan, C.-J., Tsai, M.-C., Rick, J., Su, W.-N., Lee, J.-F., Hwang, B.-J., 2016. Visible light responsive noble metal-free nanocomposite of V-doped TiO_2 nanorod with highly reduced graphene oxide for enhanced solar H₂ production. Int. J. Hydrogen Energy 41, 6752–6762.

Alkaim, A.F., Kandiel, T.A., Hussein, F.H., Dillert, R., Bahnemann, D.W., 2013. Solvent-free hydrothermal synthesis of anatase TiO_2 nanoparticles with enhanced photocatalytic hydrogen production activity. Appl. Catal. A 466, 32–37.

Anasori, B., Lukatskaya, M.R., Gogotsi, Y., 2017. 2D metal carbides and nitrides (MXenes) for energy storage. Nat. Rev. Mater. 2, 16098.

Andoshe, D.M., Choi, S., Shim, Y.-S., Lee, S.H., Kim, Y., Moon, C.W., Kim, D.H., Lee, S.Y., Kim, T., Park, H.K., 2016. A wafer-scale antireflective protection layer of solution-processed TiO_2 nanorods for high performance silicon-based water splitting photocathodes. J. Mater. Chem. A 4, 9477–9485.

Andoshe, D.M., Yim, K., Sohn, W., Kim, C., Kim, T.L., Kwon, K.C., Hong, K., Choi, S., Moon, C.W., Hong, S.-P., 2018. One-pot synthesis of sulfur and nitrogen codoped titanium dioxide nanorod arrays for superior photoelectrochemical water oxidation. Appl. Catal. B 234, 213–222.

Antwi-Baah, R., Liu, H., 2018. Recent hydrophobic metal-organic frameworks and their applications. Materials 11, 2250.

Avtar, R., Sahu, N., Aggarwal, A.K., Chakraborty, S., Kharrazi, A., Yunus, A.P., Dou, J., Kurniawan, T.A., 2019. Exploring renewable energy resources using remote sensing and GIS—A review. Resources 8, 149.

Bai, J., Han, Q., Cheng, Z., Qu, L., 2018. Wall-mesoporous graphitic carbon nitride nanotubes for efficient photocatalytic hydrogen evolution. Chem. Asian J. 13, 3160–3164.

Bakar, S.A., Ribeiro, C., 2016. Rapid and morphology controlled synthesis of anionic s-doped TiO_2 photocatalysts for the visible-light-driven photodegradation of organic pollutants. RSC Adv. 6, 36516–36527.

Bala, S., Mondal, I., Goswami, A., Pal, U., Mondal, R., 2015. Co-MOF as a sacrificial template: Manifesting a new Co_3O_4/TiO_2 system with a p–n heterojunction for photocatalytic hydrogen evolution. J. Mater. Chem. A 3, 20288–20296.

Banerjee, B., Amoli, V., Maurya, A., Sinha, A.K., Bhaumik, A., 2015. Green synthesis of Pt-doped TiO_2 nanocrystals with exposed (001) facets and mesoscopic void space for photo-splitting of water under solar irradiation. Nanoscale 7, 10504–10512.

Baykara, S.Z., 2018. Hydrogen: A brief overview on its sources, production and environmental impact. Int. J. Hydrogen Energy 43, 10605–10614.

Cao, S., Yu, J., 2014. g-C_3N_4-based photocatalysts for hydrogen generation. J. Phys. Chem. Lett. 5, 2101–2107.

Catapan, R.C., Cancino, L.R., Oliveira, A.A., Schwarz, C.O., Nitschke, H., Frank, T., 2018. Potential for onboard hydrogen production in an direct injection ethanol fueled spark ignition engine with EGR. Fuel 234, 441–446.

Chaemchuen, S., Kabir, N.A., Zhou, K., Verpoort, F., 2013. Metal–organic frameworks for upgrading biogas via CO_2 adsorption to biogas green energy. Chem. Soc. Rev. 42, 9304–9332.

Chen, Z., Fan, T.-T., Yu, X., Wu, Q.-L., Zhu, Q.-H., Zhang, L.-Z., Li, J.-H., Fang, W.-P., Yi, X.-D., 2018. Gradual carbon doping of graphitic carbon nitride towards metal-free visible light photocatalytic hydrogen evolution. J. Mater. Chem. A 6, 15310–15319.

Chen, X., Liu, L., Peter, Y.Y., Mao, S.S., 2011. Increasing solar absorption for photocatalysis with black hydrogenated titanium dioxide nanocrystals. Science 331, 746–750.

Chen, J., Qiu, F., Xu, W., Cao, S., Zhu, H., 2015. Recent progress in enhancing photocatalytic efficiency of TiO_2-based materials. Appl. Catal. A 495, 131–140.

Chen, J., Cen, J., Xu, X., Li, X., 2016b. The application of heterogeneous visible light photocatalysts in organic synthesis. Catal. Sci. Technol. 6, 349–362.

Chen, Y.-F., Tan, L.-L., Liu, J.-M., Qin, S., Xie, Z.-Q., Huang, J.-F., Xu, Y.-W., Xiao, L.-M., Su, C.-Y., 2017. Calix[4]arene based dye-sensitized Pt@UiO-66-NH$_2$ metal-organic framework for efficient visible-light photocatalytic hydrogen production. Appl. Catal. B 206, 426–433.

Chen, H., Tang, M., Rui, Z., Wang, X., Ji, H., 2016a. ZnO modified TiO_2 nanotube array supported Pt catalyst for HCHO removal under mild conditions. Catal. Today 264, 23–30.

Cheng, H., Wang, J., Zhao, Y., Han, X., 2014. Effect of phase composition, morphology, and specific surface area on the photocatalytic activity of TiO_2 nanomaterials. RSC Adv. 4, 47031–47038.

Dekrafft, K.E., Wang, C., Lin, W., 2012. Metal-organic framework templated synthesis of Fe_2O_3/TiO_2 nanocomposite for hydrogen production. Adv. Mater. 24, 2014–2018.

Dholam, R., Patel, N., Adami, M., Miotello, A., 2009. Hydrogen production by photocatalytic water-splitting using Cr-or Fe-doped TiO_2 composite thin films photocatalyst. Int. J. Hydrogen Energy 34, 5337–5346.

Fang, J., Cao, S.-W., Wang, Z., Shahjamali, M.M., Loo, S.C.J., Barber, J., Xue, C., 2012. Mesoporous plasmonic Au–TiO_2 nanocomposites for efficient visible-light-driven photocatalytic water reduction. Int. J. Hydrogen Energy 37, 17853–17861.

Fang, X.-X., Ma, L.-B., Liang, K., Zhao, S.-J., Jiang, Y.-F., Ling, C., Zhao, T., Cheang, T.-Y., Xu, A.-W., 2019. The doping of phosphorus atoms into graphitic carbon nitride for highly enhanced photocatalytic hydrogen evolution. J. Mater. Chem. A 7, 11506–11512.

Farha, O.K., Eryazici, I., Jeong, N.C., Hauser, B.G., Wilmer, C.E., Sarjeant, A.A., Snurr, R.Q., Nguyen, S.T., Yazaydın, A.O.z.r., Hupp, J.T., 2012. Metal–organic framework materials with ultra-high surface areas: Is the sky the limit?. J. Am. Chem. Soc. 134, 15016–15021.

Fujishima, A., Honda, K., 1972. Electrochemical photolysis of water at a semiconductor electrode. Nature 238, 37–38.

Gao, Q., Si, F., Zhang, S., Fang, Y., Chen, X., Yang, S., 2019. Hydrogenated F-doped TiO_2 for photocatalytic hydrogen evolution and pollutant degradation. Int. J. Hydrogen Energy 44, 8011–8019.

Gomes Silva, C., Luz, I., Llabrés i Xamena, F.X., Corma, A., García, H., 2010. Water stable Zr–benzenedicarboxylate metal–organic frameworks as photocatalysts for hydrogen generation. Chem.: Eur J. 16, 11133–11138.

Guayaquil-Sosa, J., Serrano-Rosales, B., Valadés-Pelayo, P., De Lasa, H., 2017. Photocatalytic hydrogen production using mesoporous TiO_2 doped with Pt. Appl. Catal. B 211, 337–348.

Guo, Y., Liu, Q., Li, Z., Zhang, Z., Fang, X., 2018. Enhanced photocatalytic hydrogen evolution performance of mesoporous

graphitic carbon nitride Co-doped with potassium and iodine. Appl. Catal. B 221, 362–370.

Hantanasirisakul, K., Gogotsi, Y., 2018. Electronic and optical properties of 2D transition metal carbides and nitrides (MXenes). Adv. Mater. 30, 1804779.

Haruta, M., 1997. Size-and support-dependency in the catalysis of gold. Catal. Today 36, 153–166.

Haryanto, A., Fernando, S., Murali, N., Adhikari, S., 2005. Current status of hydrogen production techniques by steam reforming of ethanol: A review. Energy Fuels 19, 2098–2106.

He, J., Yan, Z., Wang, J., Xie, J., Jiang, L., Shi, Y., Yuan, F., Yu, F., Sun, Y., 2013. Significantly enhanced photocatalytic hydrogen evolution under visible light over CdS embedded on metal–organic frameworks. Chem. Commun. 49, 6761–6763.

Hong, S.-P., Park, J.S.M., Bhat, S., Lee, T.H., Lee, S.A., Hong, K., Choi, M.-J., Shokouhimehr, M., Jang, H.W., 2018. Comprehensive study on the morphology control of TiO2 nanorods on foreign substrates by the hydrothermal method. Cryst. Growth Des. 18, 6504–6512.

Hou, H., Gao, F., Shang, M., Wang, L., Zheng, J., Yang, Z., Xu, J., Yang, W., 2017. Enhanced visible-light responsive photocatalytic activity of N-doped TiO_2 thoroughly mesoporous nanofibers. J. Mater. Sci. Mater. Electron. 28, 3796–3805.

Hou, Y., Laursen, A.B., Zhang, J., Zhang, G., Zhu, Y., Wang, X., Dahl, S., Chorkendorff, I., 2013. Layered nanojunctions for hydrogen-evolution catalysis. Angew. Chem. Int. Ed. 52, 3621–3625.

Hou, X., Wang, C.-W., Zhu, W.-D., Wang, X.-Q., Li, Y., Wang, J., Chen, J.-B., Gan, T., Hu, H.-Y., Zhou, F., 2014. Preparation of nitrogen-doped anatase TiO_2 nanoworm/nanotube hierarchical structures and its photocatalytic effect. Solid State Sci. 29, 27–33.

Huang, J., Li, G., Zhou, Z., Jiang, Y., Hu, Q., Xue, C., Guo, W., 2018. Efficient photocatalytic hydrogen production over Rh and Nb codoped TiO_2 nanorods. Chem. Eng. J. 337, 282–289.

Hussein, A.M., Mahoney, L., Peng, R., Kibombo, H., Wu, C.-M., Koodali, R.T., Shende, R., 2013. Mesoporous coupled ZnO/TiO_2 photocatalyst nanocomposites for hydrogen generation. J. Renew. Sustain. Ener. 5. 033118.

Im, J.S., Park, S.-J., Kim, T., Lee, Y.-S., 2009. Hydrogen storage evaluation based on investigations of the catalytic properties of metal/metal oxides in electrospun carbon fibers. Int. J. Hydrogen Energy 34, 3382–3388.

Iwase, A., Ng, Y.H., Ishiguro, Y., Kudo, A., Amal, R., 2011. Reduced graphene oxide as a solid-state electron mediator in Z-scheme photocatalytic water splitting under visible light. J. Am. Chem. Soc. 133, 11054–11057.

Jafari, T., Moharreri, E., Amin, A., Miao, R., Song, W., Suib, S., 2016. Photocatalytic water splitting—the untamed dream: A review of recent advances. Molecules 21, 900.

Jayaramulu, K., Toyao, T., Ranc, V., Rösler, C., Petr, M., Zboril, R., Horiuchi, Y., Matsuoka, M., Fischer, R.A., 2016. An in situ porous cuprous oxide/nitrogen-rich graphitic carbon nanocomposite derived from a metal–organic framework for visible light driven hydrogen evolution. J. Mater. Chem. A 4, 18037–18042.

Jing, D., Guo, L., 2007. WS$_2$ sensitized mesoporous TiO_2 for efficient photocatalytic hydrogen production from water under visible light irradiation. Catal. Commun. 8, 795–799.

Kandiel, T.A., Takanabe, K., 2016. Solvent-induced deposition of Cu–Ga–In–S nanocrystals onto a titanium dioxide surface for visible-light-driven photocatalytic hydrogen production. Appl. Catal. B 184, 264–269.

Khore, S.K., Tellabati, N.V., Apte, S.K., Naik, S.D., Ojha, P., Kale, B.B., Sonawane, R.S., 2017. Green sol–gel route for selective growth of 1D rutile N-TiO_2: A highly active photocatalyst for H$_2$ generation and environmental remediation under natural sunlight. RSC Adv. 7, 33029–33042.

Kim, S., Kwon, K.C., Park, J.Y., Cho, H.W., Lee, I., Kim, S.Y., Lee, J.-L., 2016. Challenge beyond graphene: Metal oxide/graphene/metal oxide electrodes for optoelectronic devices. ACS Appl. Mater. Interfaces 8, 12932–12939.

Kim, H.-I., Moon, G.-H., Monllor-Satoca, D., Park, Y., Choi, W., 2011. Solar photoconversion using graphene/TiO$_2$ composites: Nanographene shell on TiO$_2$ core versus TiO$_2$ nanoparticles on graphene sheet. J. Phys. Chem. C 116, 1535–1543.

Kočí, K., Matějů, K., Obalová, L., Krejčíková, S., Lacný, Z., Plachá, D., Čapek, L., Hospodková, A., Šolcová, O., 2010. Effect of silver doping on the TiO$_2$ for photocatalytic reduction of CO$_2$. Appl. Catal. B 96, 239–244.

Lang, Q., Chen, Y., Huang, T., Yang, L., Zhong, S., Wu, L., Chen, J., Bai, S., 2018. Graphene "bridge" in transferring hot electrons from plasmonic ag nanocubes to TiO$_2$ nanosheets for enhanced visible light photocatalytic hydrogen evolution. Appl. Catal. B 220, 182–190.

Li, X., Hartley, G., Ward, A.J., Young, P.A., Masters, A.F., Maschmeyer, T., 2015b. Hydrogenated defects in graphitic carbon nitride nanosheets for improved photocatalytic hydrogen evolution. J. Phys. Chem. C 119, 14938–14946.

Li, Z., Luan, Y., Qu, Y., Jing, L., 2015c. Modification strategies with inorganic acids for efficient photocatalysts by promoting the adsorption of O$_2$. ACS Appl. Mater. Interfaces 7, 22727–22740.

Li, L., Yan, J., Wang, T., Zhao, Z.-J., Zhang, J., Gong, J., Guan, N., 2015a. Sub-10 nm rutile titanium dioxide nanoparticles for efficient visible-light-driven photocatalytic hydrogen production. Nat. Commun. 6, 5881.

Lin, H.-Y., Shih, C.-Y., 2016. Efficient one-pot microwave-assisted hydrothermal synthesis of M (M = Cr, Ni, Cu, Nb) and nitrogen co-doped TiO$_2$ for hydrogen production by photocatalytic water splitting. J. Mol. Catal. Chem 411, 128–137.

Liu, J., Bai, H., Wang, Y., Liu, Z., Zhang, X., Sun, D.D., 2010. Self-assembling TiO$_2$ nanorods on large graphene oxide sheets at a two-phase interface and their anti-recombination in photocatalytic applications. Adv. Funct. Mater. 20, 4175–4181.

Liu, T., Chen, W., Liu, X., Zhu, J., Lu, L., 2016. Well-dispersed ultrafine nitrogen-doped TiO$_2$ with polyvinylpyrrolidone (PVP) acted as N-source and stabilizer for water splitting. J. Energy Chem. 25, 1–9.

Liu, D., Jin, Z., Bi, Y., 2017. Charge transmission channel construction between a MOF and rGO by means of Co–Mo–S modification. Catal. Sci. Technol. 7, 4478–4488.

Liu, E., Kang, L., Yang, Y., Sun, T., Hu, X., Zhu, C., Liu, H., Wang, Q., Li, X., Fan, J., 2014b. Plasmonic Ag deposited TiO$_2$ nano-sheet film for enhanced photocatalytic hydrogen production by water splitting. Nanotechnology 25. 165401.

Liu, B., Liu, L.-M., Lang, X.-F., Wang, H.-Y., Lou, X.W.D., Aydil, E.S., 2014a. Doping high-surface-area mesoporous TiO$_2$ microspheres with carbonate for visible light hydrogen production. Energy Environ. Sci. 7, 2592–2597.

Low, J., Cao, S., Yu, J., Wageh, S., 2014. Two-dimensional layered composite photocatalysts. Chem. Commun. 50, 10768–10777.

Lu, W., Wei, Z., Gu, Z.-Y., Liu, T.-F., Park, J., Park, J., Tian, J., Zhang, M., Zhang, Q., Gentle III, T., 2014. Tuning the structure and function of metal–organic frameworks via linker design. Chem. Soc. Rev. 43, 5561–5593.

Luna, A.L., Dragoe, D., Wang, K., Beaunier, P., Kowalska, E., Ohtani, B., Bahena Uribe, D., Valenzuela, M.A., Remita, H., Colbeau-Justin, C., 2017. Photocatalytic hydrogen evolution using Ni–Pd/TiO$_2$: Correlation of light absorption, charge-carrier dynamics, and quantum efficiency. J. Phys. Chem. C 121, 14302–14311.

Luo, H., Takata, T., Lee, Y., Zhao, J., Domen, K., Yan, Y., 2004. Photocatalytic activity enhancing for titanium dioxide by co-doping with bromine and chlorine. Chem. Mater. 16, 846–849.

Ma, B., Guan, P.-Y., Li, Q.-Y., Zhang, M., Zang, S.-Q., 2016. MOF-derived flower-like MoS$_2$@TiO$_2$ nanohybrids with enhanced activ-

ity for hydrogen evolution. ACS Appl. Mater. Interfaces 8, 26794–26800.

Maina, J.W., Pozo-Gonzalo, C., Kong, L., Schütz, J., Hill, M., Dumée, L.F., 2017. Metal organic framework based catalysts for CO$_2$ conversion. Mater. Horiz. 4, 345–361.

Majeed, I., Nadeem, M.A., Badshah, A., Kanodarwala, F.K., Ali, H., Khan, M.A., Stride, J.A., Nadeem, M.A., 2017. Titania supported MOF-199 derived Cu-Cu$_2$O nanoparticles: Highly efficient non-noble metal photocatalysts for hydrogen production from alcohol–water mixtures. Catal. Sci. Technol. 7, 677–686.

Mandari, K.K., Police, A.K.R., Do, J.Y., Kang, M., Byon, C., 2018. Rare earth metal Gd influenced defect sites in N doped TiO$_2$: Defect mediated improved charge transfer for enhanced photocatalytic hydrogen production. Int. J. Hydrogen Energy 43, 2073–2082.

McManamon, C., O'Connell, J., Delaney, P., Rasappa, S., Holmes, J. D., Morris, M.A., 2015. A facile route to synthesis of S-doped TiO$_2$ nanoparticles for photocatalytic activity. J. Mol. Catal. Chem. 406, 51–57.

Meriam Suhaimy, S., Lai, C., Tajuddin, H., Samsudin, E., Johan, M., 2018. Impact of TiO$_2$ nanotubes' morphology on the photocatalytic degradation of simazine pollutant. Materials 11, 2066.

Min, S., Lu, G., 2012. Sites for high efficient photocatalytic hydrogen evolution on a limited-layered MoS$_2$ cocatalyst confined on graphene sheets-the role of graphene. J. Phys. Chem. C 116, 25415–25424.

Mondal, I., Pal, U., 2016. Synthesis of MOF templated Cu/CuO@TiO$_2$ nanocomposites for synergistic hydrogen production. Phys. Chem. Chem. Phys. 18, 4780–4788.

Montoya, A.T., Gillan, E.G., 2018. Enhanced photocatalytic hydrogen evolution from transition-metal surface-modified TiO$_2$. ACS Omega 3, 2947–2955.

Ouyang, W., Munoz-Batista, M.J., Kubacka, A., Luque, R., Fernandez-Garcia, M., 2018. Enhancing photocatalytic performance of TiO$_2$ in H$_2$ evolution via Ru co-catalyst deposition. Appl. Catal. B 238, 434–443.

Pang, Y.L., Lim, S., Ong, H.C., Chong, W.T., 2014. A critical review on the recent progress of synthesizing techniques and fabrication of TiO$_2$-based nanotubes photocatalysts. Appl. Catal. A 481, 127–142.

Pang, J., Mendes, R.G., Bachmatiuk, A., Zhao, L., Ta, H.Q., Gemming, T., Liu, H., Liu, Z., Rummeli, M.H., 2019. Applications of 2D MXenes in energy conversion and storage systems. Chem. Soc. Rev. 48, 72–133.

Pao, H.-T., Tsai, C.-M., 2010. CO$_2$ emissions, energy consumption and economic growth in bric countries. Energy Policy 38, 7850–7860.

Park, Y.R., Choi, K.S., Kim, J.C., Seo, Y.S., Kim, S.Y., Kim, Y.J., Choi, W.K., Jeong, H.Y., Yang, W.S., Hong, Y.J., 2017. Graphene oxide inserted poly (n-vinylcarbazole)/vanadium oxide hole transport heterojunctions for high-efficiency quantum-dot light-emitting diodes. Adv. Mater. Interfaces 4, 1700476.

Patra, K.K., Gopinath, C.S., 2016. Bimetallic and plasmonic Ag–Au on TiO$_2$ for solar water splitting: An active nanocomposite for entire visible-light-region absorption. Chem. Cat. Chem. 8, 3294–3311.

Peng, C., Wei, P., Li, X., Liu, Y., Cao, Y., Wang, H., Yu, H., Peng, F., Zhang, L., Zhang, B., 2018. High efficiency photocatalytic hydrogen production over ternary Cu/TiO$_2$@Ti$_3$C$_2$T$_x$ enabled by low-work-function 2D titanium carbide. Nano Energy 53, 97–107.

Perera, S.D., Mariano, R.G., Vu, K., Nour, N., Seitz, O., Chabal, Y., Balkus Jr, K.J., 2012. Hydrothermal synthesis of graphene-TiO$_2$ nanotube composites with enhanced photocatalytic activity. ACS Catal. 2, 949–956.

Preethi, L., Antony, R.P., Mathews, T., Loo, S., Wong, L.H., Dash, S., Tyagi, A., 2016. Nitrogen doped anatase-rutile heterostructured nanotubes for enhanced photocatalytic hydrogen production:

Promising structure for sustainable fuel production. Int. J. Hydrogen Energy 41, 5865–5877.

Rahul, T.K., Mohan, M., Sandhyarani, N., 2018. Enhanced solar hydrogen evolution over in situ gold–platinum bimetallic nanoparticle-loaded Ti^{3+} self-doped titania photocatalysts. ACS Sustain. Chem. Eng. 6, 3049–3059.

Rather, R.A., Singh, S., Pal, B., 2017. A Cu^{+1}/Cu^0-TiO_2 mesoporous nanocomposite exhibits improved H_2 production from H_2O under direct solar irradiation. J. Catal. 346, 1–9.

Reddy, P.A.K., Reddy, P.V.L., Kim, K.-H., Kumar, M.K., Manvitha, C., Shim, J.-J., 2017. Novel approach for the synthesis of nitrogen-doped titania with variable phase composition and enhanced production of hydrogen under solar irradiation. J. Ind. Eng. Chem. 53, 253–260.

Rossetti, I., Villa, A., Compagnoni, M., Prati, L., Ramis, G., Pirola, C., Bianchi, C., Wang, W., Wang, D., 2015. CO_2 photoconversion to fuels under high pressure: Effect of TiO_2 phase and of unconventional reaction conditions. Catal. Sci. Technol. 5, 4481–4487.

Sadanandam, G., Lalitha, K., Kumari, V.D., Shankar, M.V., Subrahmanyam, M., 2013. Cobalt doped TiO_2: A stable and efficient photocatalyst for continuous hydrogen production from glycerol: Water mixtures under solar light irradiation. Int. J. Hydrogen Energy 38, 9655–9664.

Santaclara, J., Olivos-Suarez, A., du Fossé, I., Houtepen, A., Hunger, J., Kapteijn, F., Gascon, J., van der Veen, M., 2017. Harvesting the photoexcited holes on a photocatalytic proton reduction metal–organic framework. Faraday Discuss 201, 71–86.

Sood, S., Umar, A., Mehta, S.K., Kansal, S.K., 2015. Highly effective Fe-doped TiO_2 nanoparticles photocatalysts for visible-light driven photocatalytic degradation of toxic organic compounds. J. Colloid Interface Sci. 450, 213–223.

Staffell, I., Scamman, D., Abad, A.V., Balcombe, P., Dodds, P.E., Ekins, P., Shah, N., Ward, K.R., 2019. The role of hydrogen and fuel cells in the global energy system. Energy & Environ. Sci. 12, 463–491.

Sun, T., Fan, J., Liu, E., Liu, L., Wang, Y., Dai, H., Yang, Y., Hou, W., Hu, X., Jiang, Z., 2012. Fe and Ni co-doped TiO_2 nanoparticles prepared by alcohol-thermal method: Application in hydrogen evolution by water splitting under visible light irradiation. Powder Technol. 228, 210–218.

Sun, T., Liu, E., Liang, X., Hu, X., Fan, J., 2015. Enhanced hydrogen evolution from water splitting using Fe-Ni codoped and Ag deposited anatase TiO_2 synthesized by solvothermal method. Appl. Surf. Sci. 347, 696–705.

Sun, S., Zhang, J., Gao, P., Wang, Y., Li, X., Wu, T., Wang, Y., Chen, Y., Yang, P., 2017. Full visible-light absorption of TiO_2 nanotubes induced by anionic S_2^{2-} doping and their greatly enhanced photocatalytic hydrogen production abilities. Appl. Catal. B: Environ. 206, 168–174.

Taherinia, M., Nasiri, M., Abedini, E., Pouretedal, H.R., 2019. Influence of calcination temperature and solvent of titanium precursor on the photocatalytic activity of N-doped TiO_2 nanoparticles in H_2 evolution under visible radiation. Environ. Dev. Sustainability 21, 1963–1975.

Tanigawa, S., Irie, H., 2016. Visible-light-sensitive two-step overall water-splitting based on band structure control of titanium dioxide. Appl. Catal. B 180, 1–5.

Tusek, J., Suban, M., 2000. Experimental research of the effect of hydrogen in argon as a shielding gas in arc welding of high-alloy stainless steel. Int. J. Hydrogen. Energy 25, 369–376.

Valden, M., Lai, X., Goodman, D.W., 1998. Onset of catalytic activity of gold clusters on titania with the appearance of nonmetallic properties. Science 281, 1647–1650.

Wang, H., Peng, R., Hood, Z.D., Naguib, M., Adhikari, S.P., Wu, Z., 2016. Titania composites with 2D transition metal carbides as photocatalysts for hydrogen production under visible-light irradiation. Chem. Sus. Chem. 9, 1490–1497.

Wang, H., Huang, G., Chen, Z., Li, W., 2018. Carbon self-doped carbon nitride nanosheets with enhanced visible-light photocatalytic hydrogen production. Catalysts 8, 366.

Wang, Y., Wang, X., Antonietti, M., 2012. Polymeric graphitic carbon nitride as a heterogeneous organocatalyst: From photochemistry to multipurpose catalysis to sustainable chemistry. Angew. Chem. Int. Ed. 51, 68–89.

Wang, Z., Yang, C., Lin, T., Yin, H., Chen, P., Wan, D., Xu, F., Huang, F., Lin, J., Xie, X., 2013. H-doped black titania with very high solar absorption and excellent photocatalysis enhanced by localized surface plasmon resonance. Adv. Funct. Mater. 23, 5444–5450.

Wen, M., Cui, Y., Kuwahara, Y., Mori, K., Yamashita, H., 2016. Non-noble-metal nanoparticle supported on metal–organic framework as an efficient and durable catalyst for promoting H_2 production from ammonia borane under visible light irradiation. ACS Appl. Mater. Interfaces 8, 21278–21284.

Wu, F., Hu, X., Fan, J., Liu, E., Sun, T., Kang, L., Hou, W., Zhu, C., Liu, H., 2013a. Photocatalytic activity of Ag/TiO_2 nanotube arrays enhanced by surface plasmon resonance and application in hydrogen evolution by water splitting. Plasmonics 8, 501–508.

Wu, N.-L., Lee, M.-S., 2004. Enhanced TiO_2 photocatalysis by Cu in hydrogen production from aqueous methanol solution. Int. J. Hydrogen Energy 29, 1601–1605.

Wu, B., Liu, D., Mubeen, S., Chuong, T.T., Moskovits, M., Stucky, G.D., 2016a. Anisotropic growth of TiO_2 onto gold nanorods for plasmon-enhanced hydrogen production from water reduction. J. Am. Chem. Soc. 138, 1114–1117.

Wu, J., Lu, S., Ge, D., Zhang, L., Chen, W., Gu, H., 2016b. Photocatalytic properties of Pd/TiO_2 nanosheets for hydrogen evolution from water splitting. RSC Adv. 6, 67502–67508.

Wu, X., Yin, S., Dong, Q., Guo, C., Li, H., Kimura, T., Sato, T., 2013b. Synthesis of high visible light active carbon doped TiO_2 photocatalyst by a facile calcination assisted solvothermal method. Appl. Catal. B 142, 450–457.

Xia, W., Mahmood, A., Zou, R., Xu, Q., 2015. Metal–organic frameworks and their derived nanostructures for electrochemical energy storage and conversion. Energy Environ. Sci. 8, 1837–1866.

Xiang, Q., Yu, J., Jaroniec, M., 2012. Synergetic effect of MoS_2 and graphene as cocatalysts for enhanced photocatalytic H_2 production activity of TiO_2 nanoparticles. J. Am. Chem. Soc. 134, 6575–6578.

Xie, M.-Y., Su, K.-Y., Peng, X.-Y., Wu, R.-J., Chavali, M., Chang, W.-C., 2017. Hydrogen production by photocatalytic water-splitting on Pt-doped TiO_2–ZnO under visible light. J. Taiwan Inst. Chem. E.70, 161–167.

Yamazaki, Y., Azami, K., Katoh, R., Yamazaki, S., 2018. Developing active TiO_2 nanorods by examining the influence of morphological changes from nanorods to nanoparticles on photocatalytic activity. ACS Appl. Nano Mater. 1, 5927–5935.

Yan, B., Zhang, L., Tang, Z., Al-Mamun, M., Zhao, H., Su, X., 2017. Palladium-decorated hierarchical titania constructed from the metal-organic frameworks NH_2-MIL-125 (Ti) as a robust photocatalyst for hydrogen evolution. Appl. Catal. B 218, 743–750.

Yang, C., Wang, Z., Lin, T., Yin, H., Lü, X., Wan, D., Xu, T., Zheng, C., Lin, J., Huang, F., 2013. Core-shell nanostructured "black" rutile titania as excellent catalyst for hydrogen production enhanced by sulfur doping. J. Am. Chem. Soc. 135, 17831–17838.

Yang, Y., Ye, K., Cao, D., Gao, P., Qiu, M., Liu, L., Yang, P., 2018. Efficient charge separation from F–selective etching and doping of anatase-TiO2 001 for enhanced photocatalytic hydrogen production. ACS Appl. Mater. Interfaces 10, 19633–19638.

Yoon, J.W., Kim, D.H., Kim, J.-H., Jang, H.W., Lee, J.-H., 2019. NH_2-MIL-125 (Ti)/TiO_2 nanorod heterojunction photoanodes for efficient photoelectrochemical water splitting. Appl. Catal. B: Environ. 244, 511–518.

Zhang, J., Jin, X., Morales-Guzman, P.I., Yu, X., Liu, H., Zhang, H., Razzari, L., Claverie, J.P., 2016. Engineering the absorption and field enhancement properties of Au–TiO_2 nanohybrids via whis-

pering gallery mode resonances for photocatalytic water splitting. ACS Nano 10, 4496–4503.

Zhang, X.-Y., Li, H.-P., Cui, X.-L., Lin, Y., 2010. Graphene/TiO$_2$ nanocomposites: Synthesis, characterization and application in hydrogen evolution from water photocatalytic splitting. J. Mater. Chem. 20, 2801–2806.

Zhang, W., Wang, S., Li, J., Yang, X., 2015a. Photocatalytic hydrogen production from methanol aqueous solution under visible-light using Cu/S–TiO$_2$ prepared by electroless plating method. Catal. Commun. 59, 189–194.

Zhang, J., Yu, J., Jaroniec, M., Gong, J.R., 2012. Noble metal-free reduced graphene oxide-Zn$_x$Cd$_{1-x}$S nanocomposite with enhanced solar photocatalytic H$_2$-production performance. Nano Lett. 12, 4584–4589.

Zhang, Z.-M., Zhang, T., Wang, C., Lin, Z., Long, L.-S., Lin, W., 2015b. Photosensitizing metal–organic framework enabling visible-light-driven proton reduction by a wells–dawson-type polyoxometalate. J. Am. Chem. Soc. 137, 3197–3200.

Zhen, W., Ma, J., Lu, G., 2016. Small-sized Ni(1 1 1) particles in metal-organic frameworks with low over-potential for visible photocatalytic hydrogen generation. Appl. Catal. B 190, 12–25.

Zheng, X., Kuang, Q., Yan, K., Qiu, Y., Qiu, J., Yang, S., 2013. Mesoporous TiO$_2$ single crystals: Facile shape-, size-, and phase-controlled growth and efficient photocatalytic performance. ACS Appl. Mater. Interfaces 5, 11249–11257.

Zheng, Q., Liu, X., Xu, H., Cheung, M.-S., Choi, Y.-W., Huang, H.-C., Lei, H.-Y., Shen, X., Wang, Z., Wu, Y., 2018. Sliced graphene foam films for dual-functional wearable strain sensors and switches. Nanoscale Horiz. 3, 35–44.

Zhou, W., Li, W., Wang, J.-Q., Qu, Y., Yang, Y., Xie, Y., Zhang, K., Wang, L., Fu, H., Zhao, D., 2014. Ordered mesoporous black TiO$_2$ as highly efficient hydrogen evolution photocatalyst. J. Am. Chem. Soc. 136, 9280–9283.

Zhu, Z., Chen, J.-Y., Su, K.-Y., Wu, R.-J., 2016. Efficient hydrogen production by water-splitting over Pt-deposited C-HS–TiO$_2$ hollow spheres under visible light. J. Taiwan. Inst. Chem. E. 60, 222–228.

Zhu, Y., Ling, Q., Liu, Y., Wang, H., Zhu, Y., 2015. Photocatalytic H$_2$ evolution on MoS$_2$-TiO$_2$ catalysts synthesized via mechanochemistry. Phys. Chem. Chem. Phys. 17, 933–940.

Zhu, B., Zou, R., Xu, Q., 2018. Metal–organic framework based catalysts for hydrogen evolution. Adv. Energy Mater. 8, 1801193.